

# Statistical tools for seed bank detection

JOCHEN BLATH<sup>1</sup>, EUGENIO BUZZONI<sup>1</sup>, JERE KOSKELA<sup>2</sup>, and MAITE WILKE-BERENQUER<sup>3</sup>

<sup>1</sup>Institut für Mathematik, Technische Universität Berlin, Straße des 17. Juni 136, 10623 Berlin, Germany.

<sup>2</sup>Statistics Department, University of Warwick, Coventry CV4 7AL, UK.

<sup>3</sup>Fakultät für Mathematik, Ruhr-Universität Bochum, Universitätsstraße 150, 44801 Bochum, Germany

## Abstract

In this article, we derive statistical tools to analyze and distinguish the patterns of genetic variability produced by classical and recent population genetic models related to seed banks. In particular, we are concerned with models described by the Kingman coalescent ( $K$ ), models exhibiting so-called weak seed banks described by a time-changed Kingman coalescent ( $W$ ), models with so-called strong seed bank described by the seed bank coalescent ( $S$ ) and the classical two-island model by Wright, described by the structured coalescent ( $TI$ ). As the presence of a (strong) seed bank should stratify a population, we expect it to produce a signal roughly comparable to the presence of population structure.

We begin with a brief analysis of Wright's  $F_{ST}$ , which is a classical but crude measure for population structure, followed by a derivation of the expected site frequency spectrum in the infinite sites model based on 'phase-type distribution calculus' as recently discussed by Hobolth et al. (2019).

Both  $F_{ST}$  and the SFS can be readily computed under various population models, they discard statistical signal. Hence we also derive exact likelihoods for the full sampling probabilities, which can be achieved via recursions and a Monte Carlo scheme both in the infinite alleles and the infinite sites model. We employ a pseudo-marginal Metropolis-Hastings algorithm of Andrieu and Roberts (2009) to provide a method for simultaneous model selection and parameter inference under the so-called infinitely-many sites model, which is the most relevant in real applications. It turns out that this full likelihood method can reliably distinguish among the model classes ( $K, W$ ), ( $S$ ) and ( $TI$ ) on the basis of simulated data even from moderate sample sizes. It is also possible to infer mutation rates, and in particular determine whether mutation is taking place in the (strong) seed bank.

*2010 Mathematics Subject Classification:* Primary 92D10.

**Keywords:** Seed bank, dormancy, seed bank coalescent, two island model, sampling formula, model selection, inference, pseudo-marginal Metropolis-Hastings.

# 1 Introduction and basic models

## 1.1 Seed banks in population genetics

Seed banks, that is, reservoirs of dormant individuals that can potentially be resuscitated in the future, are common in many communities of macroscopic (e.g. plants) and microscopic (e.g. bacteria) organisms. They extend the persistence of genotypes and are important for the diversity and functioning of populations. In particular, microbial dormancy is common in a range of ecosystems, and there is evidence that the ecology and evolution of microbial communities are strongly influenced by seed bank dynamics. It has been observed that more than 90% of microbial biomass in soil is metabolically inactive. See [LJ11] and [SL18] for recent overviews on this subject.

In the context of population genetics, seed banks have a significant influence on classical evolutionary forces such as selection and genetic drift. For example, seed banks can counteract the effect of genetic drift, and lead to stratification of the population. However, the development of a comprehensive population genetic theory incorporating seed banks is still in its early stages. See [SL18] for a review of the current literature and an assessment of relevant open questions. While some basic mathematical models have been derived and predict unique patterns of genetic variability in idealized scenarios [KKL01, LJ11, ZT12, BGE<sup>+</sup>15, BGKW16, dHP17], statistical tools to infer the presence of ‘weak’ or ‘strong’ seed banks are still largely missing.

The aim of this article is to provide basic statistical theory to analyze patterns of population structure and genetic variability produced by seed banks, following the recently introduced models mentioned above. We will also provide tools for parameter estimation and model selection based on genetic data. Notably, we will provide comparisons between patterns of variability under seed banks, and classical models of population structure as treated in [Her94]. Both model classes can be expected to predict somewhat similar patterns of diversity, and we will study the extent to which sequence data can differentiate between them. This extends earlier studies [TLL<sup>+</sup>11, BGE<sup>+</sup>15], where seed banks were compared to classical, panmictic models.

Before deriving such tools, we begin with a brief review of some relevant population genetic models with and without seed banks.

## 1.2 Population models

**Kingman’s coalescent (K).** The standard model of genetic ancestry in the absence of a seed bank is the *coalescent* (or *Kingman’s coalescent*) [Kin82], which describes ancestries of samples of size  $n \in \mathbb{N}$  from a large selectively neutral, panmictic population of size  $N \gg n$  following e.g. a Wright-Fisher model. Measuring time in units of  $N$  and tracing the ancestry of a sample of size  $n \ll N$  backwards in time results in a coalescent process  $\Pi^n$  in which each pair of lineages merges to a common ancestor independently at rate 1 as  $N \rightarrow \infty$ . A rooted ancestral tree is formed once the most recent common ancestor of the whole sample is reached. We denote this scenario by K. This model is currently the standard null model in population genetics (see e.g. [Wak09] for an introduction) and arises from a large class of population models.

**‘Weak’ seed banks and delayed coalescents (W).** The basic coalescent model was extended in [KKL01] to incorporate a *‘weak’ seed bank effect*. In this model, an individual does not always inherit its genetic material from a parent in the previous generation, but rather from a parent that was alive a random number of generations ago. The random separation is assumed to have mean  $\beta^{-1}$  for some  $\beta \in (0, 1]$ . Again, after measuring time in units of  $N$  and tracing the ancestry of a sample of size  $n \ll N$  as above, it can be shown that the genealogy is still given by a coalescent, but now each pair of lineages merges to a common ancestor independently with rate  $\beta^2$ , as opposed to 1. Thus, the effect of the seed bank is to stretch the branches of the Kingman coalescent by a constant factor [KKL01, BGKS13]. We call the corresponding coalescent a ‘delayed coalescent’ and denote this ‘weak’ seed bank scenario by **W**. It should be noted that the overall topological tree structure is identical to that under Kingman’s coalescent. Thus, for example, the normalized frequency spectrum of a sample in the infinitely many sites model remains unchanged [BGE<sup>+</sup>15], and in fact the delayed coalescent with mean delay  $\beta^{-1}$  and population-rescaled mutation rate  $u > 0$  is statistically identical to Kingman’s coalescent with population-rescaled mutation rate  $u/\beta^2$ . Nevertheless, the seed bank does have potentially important consequences e.g. for the estimation of effective population size and mutation rates in the presence of prior information, or some other means of resolving the lack of identifiability.

**‘Strong’ seed banks and the ‘seed bank coalescent’ (S).** The recent model in [BGKW16] extends the Wright Fisher framework to a model with a classical ‘active’ population of size  $N$  and a separate ‘seed bank’ of comparable size  $M := \lfloor N/K \rfloor$ , for some  $K > 0$ , allowing for ‘migration’ (of a fraction of  $\lfloor c/N \rfloor$  individuals) between the two subpopulations. The active population follows a Wright-Fisher model, while the dormant population in the seed bank persists without reproducing. This model can be seen as a mathematical formalization of the concept in [LJ11, Figure 2]. The age structure in the resulting seed bank is geometric with mean of order  $N$ , which means that seeds can remain viable in the seed bank for  $O(N)$  generations. Considering samples of size  $n^{(1)} \ll N$  and  $n^{(2)} \ll N$  from the active and dormant population, respectively, and again measuring time in units of  $N$  as before, the genealogy is now described by the so-called *seed bank coalescent* [BGKW16], in which active lineages fall dormant at rate  $c$  or coalesce at rate 1 per pair, and dormant lines resuscitate at rate  $cK$ , but do not coalesce. Thus, the properties of the ancestral process are drastically changed, and we speak of a *strong seed bank*, denoting this scenario by **S**. The *seed bank coalescent* features a very different site frequency spectrum compared to the classical (**K**) and weak seed bank (**W**) scenarios [BGE<sup>+</sup>15].

**The two island model and the structured coalescent (TI).** Having modeled a strong seed bank as a separate population linked to the active one via migration, it is natural to investigate its relation to Wright’s two island model [Her94, Wak09]. In the simplest case (which we assume throughout) there are two populations (1 and 2) of respective sizes  $N$  and  $M = \lfloor N/K \rfloor$ , with a fixed fraction of  $\lfloor c/N \rfloor$  individuals migrating both from 1 to 2 and from 2 to 1 in every generation. With time measured in units of  $N \rightarrow \infty$  generations, considering sample sizes  $n^{(1)} \ll N$  from island 1 and

$n^{(2)} \ll M$  from island 2, this model gives rise to a similar ancestral process as the strong seed bank coalescent except that all pairs of lineages in population 2 may also merge to a common ancestor independently with rate  $1/K$ . We denote this scenario by **TI**. The resulting ancestral process is the *structured coalescent* [Her94, Not90], which describes the ancestry of a geographically structured population with migration.

**Distinguishing the scenarios K, W, S, and TI.** In this article we investigate the extent to which genetic data can distinguish between models **K**, **W**, **S**, and **TI** outlined above. All four scenarios are a priori plausible as null models for certain real populations experiencing dormancy. In [TLL<sup>+</sup>11], the authors studied two species of wild tomato (*S. chilense* and *S. peruvianum*), and inferred average seed bank delays of 9 and 12 generations, respectively. Estimates of corresponding effective population sizes are  $O(10^5)$  [ASS07], which suggests that scenario **W** is appropriate in this context. On the other hand, dormant bacteria have been observed to remain viable for millions of years [VRP00], which suggests that the strong seed bank could be relevant. When bacterial communities sustain a stable reservoir of dormant types, in which individuals may switch (that is, *migrate*) between both reservoirs with a certain fixed rate, as outlined in [LJ11], model **S** seems appropriate. In fact, a stable reservoir of dormant individuals automatically requires periods of individual dormancy which are on the order of the active effective population size ([BGE<sup>+</sup>15]). These considerations highlight the need to distinguish the two types of seed banks from data in cases where the presence or size of a seed bank or the typical period of dormancy are uncertain. It is also of interest to distinguish the signal of (strong) seed banks from geographic structure, which could in principle produce similar patterns of stratification in the population.

### 1.3 Mutation models and key statistical quantities

We consider three popular models of genetic diversity and mutation: the finite alleles model (**FAM**) (which we take to be the two alleles model for brevity, but our results generalize to any finite number of alleles), the infinite alleles model (**IAM**), and the infinite sites model (**ISM**), each of which we outline below. We also consider several classical statistical quantities: the sample heterozygosity and Wright's  $F_{ST}$  [Wri51], the site frequency spectrum (**SFS**), and the full sampling distribution. These measures are informative about the underlying coalescent scenario, and suited to the different mutation models, to varying degrees. They also differ in the extent to which they are tractable. The sample heterozygosity, Wright's  $F_{ST}$  and the (normalized) **SFS** discard statistical signal, but are readily computed (at least numerically) in most settings. The likelihood function obtained from the sampling distribution fully captures the statistical signal in a data set, but is available for coalescent processes only via computationally intensive Monte Carlo schemes. Our results clarify when computationally cheaper summary statistics suffice to distinguish between models, and when the full likelihood is needed.

**The infinite alleles model (IAM).** Given a coalescent tree distributed according to any of the models introduced above, a sample of genetic data from the infinite

alleles model is generated by assigning an arbitrary allele to the most recent common ancestor, and simulating mutations along the branches of the coalescent tree with population-rescaled mutation rate  $u > 0$  for the branches in the first (and possibly only) population and  $u' \geq 0$  in the second population, respectively the seed bank in the model **TI** and **S**. Each mutation results in a new (parent-independent) allele that has never existed in the population before, and alleles are inherited along lineages in the absence of mutation. In the cases **K** and **W**, a sample of size  $n \in \mathbb{N}$  is then described by a tuple of length  $n$ ,  $\mathbf{n} := (n_1, \dots, n_n)$ , in which  $n_i$  is the number of lineages carrying allele  $i$  (in some fixed but arbitrary ordering of observed alleles). Note that  $n_1 + \dots + n_n = n$ , where the vector is padded with zero entries if fewer than  $n$  distinct alleles are observed for notational convenience. In the cases **S** and **TI**, we need to distinguish lineages from the two sub-populations (active and dormant resp. two islands). We consider a sample of size  $n := n^{(1)} + n^{(2)}$  (where  $n^{(i)}$  is the sample size on sub-population/island  $i$ ) by the pair  $(\mathbf{n}^{(1)}, \mathbf{n}^{(2)})$ , where both tuples together are of length  $n$  and  $n_j^{(i)}$  counts the number of  $j$  alleles on island  $i$ .

The (somewhat out-dated) infinite alleles model is appropriate when the data is uninformative enough that it is possible to discern when two alleles are different, but no further detail is available, such as is the case for electrophoresis data [HL66].

**The finite alleles model (FAM).** Here, we consider a finite set of possible alleles, which we identify with  $\{1, \dots, d\}$ . The type of the most recent common ancestor is sampled from some probability mass function  $\rho = (\rho_1, \dots, \rho_d)$ , and mutations occur along the branches of the coalescent tree at rate  $u$ , resp.  $u'$  as before. At a mutation event, a new allele is sampled from a  $d \times d$  stochastic matrix  $P$ , and alleles are inherited along branches in the absence of mutation as before. Using similar notation as for the IAM, under **K** and **W** a sample of size  $n$  is described by a tuple  $\mathbf{n} := (n_1, \dots, n_d)$ , whereas under **S** and **TI**, a sample of size  $n := n^{(1)} + n^{(2)}$  is described by a pair  $(\mathbf{n}^{(1)}, \mathbf{n}^{(2)})$  of tuples of allele frequencies, each of length  $d$ . In this article, we take  $d = 2$ , and set  $u_2 := uP_{12}$  as well as  $u_1 := uP_{21}$  for notational brevity (and define  $u'_1$  and  $u'_2$  analogously).

The finite alleles model is much richer than the infinite alleles model, but it is also less tractable. The main difficulty is the possibility of back-mutations, which are lineages that mutate and later revert back to their original allele via a reverse mutation. A compromise between these two extremes is the infinite sites model, often suitable to treat real DNA sequence data.

**The infinite sites model (ISM).** In this model we identify the locus with the unit interval  $[0, 1]$ . Mutations, which continue to occur on the branches of the coalescent tree with rate  $u$ , resp.  $u'$ , are assumed to occur at distinct sites on the locus, and are inherited along the branches of the tree so that the allele of an individual is the list of all mutations along its ancestral line. Thus, the whole history of mutations up to the root is retained. Under **S** and **TI**, a sample of size  $n := n^{(1)} + n^{(2)}$  is specified by the triple  $(\mathbf{t}, \mathbf{n}^{(1)}, \mathbf{n}^{(2)})$ , where  $\mathbf{t} := (t_1, \dots, t_d)$  is the list of all observed mutations, and  $n_j^{(i)}$  is the observed frequency of allele  $t_j$  in population  $i$ . In the simpler cases **K**

and **W**, it suffices to consider  $(\mathbf{t}, \mathbf{n})$ . For details on this parametrization of the infinite sites model and its relation to coalescent models see e.g. [BB08].

Note that when incorporating mutation in the above models, the classical Watterson estimate will depend strongly on the chosen coalescent model. Further, in scenarios **TI** and **S**, we will allow the overall mutation rate to differ between active and dormant lineages. An interesting question in this respect is to decide whether mutations take place on dormant lineages in nature, perhaps at a reduced rate [SL18].

**Diffusion models.** It is well known that all four coalescent models are dual to their respective *Wright-Fisher diffusions*, the exact form of which depends on the accompanying mutation model. The two allele, two island Wright-Fisher diffusion solves the system of SDEs

$$\begin{aligned} dX(t) &= [u_2(1 - X(t)) - u_1X(t) + c(Y(t) - X(t))]dt \\ &\quad + \alpha\sqrt{X(t)(1 - X(t))}dB(t), \\ dY(t) &= [u'_2(1 - Y(t)) - u'_1Y(t) + Kc(X(t) - Y(t))]dt \\ &\quad + \alpha'\sqrt{Y(t)(1 - Y(t))}dB'(t), \end{aligned} \tag{1}$$

with initial value  $(X(0), Y(0)) = (x, y) \in [0, 1]^2$ , where  $\alpha, \alpha'$  are effective population sizes, and  $\{B_t\}, \{B'_t\}$  are independent Brownian motions. Duals to scenarios **K**, **W**, and **S** can be recovered as special cases: for **K** we set  $\alpha = 1$  and  $c = 0$ , for **W** we take  $\alpha = \beta$  and  $c = 0$ , and for **S** we take  $\alpha = 1$  and  $\alpha' = 0$ . For scenarios **K** and **W** we also only consider the  $X$ -coordinate, and in scenario **S**, the  $X$ -coordinate corresponds to the active population, while  $Y$  is the seed bank. In each case the SDE (resp. system of SDEs) specifies an ergodic diffusion (resp. system of diffusions) with a unique stationary distribution on  $[0, 1]$  (resp.  $[0, 1]^2$ ), which we will denote by  $\mu^I$  for  $I \in \{\mathbf{K}, \mathbf{W}, \mathbf{S}, \mathbf{TI}\}$ .

Note that it is possible to derive the analogue of the Wright-Fisher diffusion also in the IAM and ISM mutation models. This will lead to measure-valued diffusions, or *Fleming-Viot processes* (cf. [EK86]), but we refrain from providing explicit technical descriptions as they are irrelevant for our inference procedures in the sequel.

## 1.4 Outline of the paper

The rest of the article is organized as follows. In Section 2 we discuss the classical summary statistics  $F_{ST}$  and site frequency spectrum (SFS). In particular, we provide methods to compute the expected site frequency spectrum based on the phase-type distribution method of Hobolth et al. [HSJB18]. We show that both statistics can distinguish the above scenarios to some extent. Since they are readily computed, they can thus serve as a plausibility check for the presence of seed banks.

In Section 3 we present recursions for the likelihood functions of samples in the IAM and ISM associated with the strong seed bank scenario (**S**), which are currently missing in the literature. These recursions are intractable in general (for large sample

sizes), so we also provide low-variance Monte Carlo schemes based on importance sampling to approximate the them.

Finally, in Section 4 we provide statistical machinery for model selection and parameter inference for all scenarios under the ISM mutation model, which is the most relevant for handling of real data. We employ a pseudo-marginal Metropolis-Hastings algorithm for simultaneous model selection and parameter inference for the different models and assess its effectiveness with simulated data sets. We also address the specific question of detection of mutation in the (strong) seed bank.

We conclude the paper with a discussion of our results in Section 5.

## 2 Classical measures of population structure

In this section, we investigate classical summary statistics for the detection of population structure, namely Wright’s  $F_{ST}$  (defined in terms of the (local and global) *sample heterozygosity* in the FAM, and *identity by descent* in the IAM and the ISM), and the (normalized) site frequency spectrum nSFS in the ISM. Unless explicitly stated otherwise, we assume strictly positive mutation rates in all (sub-)populations.

### 2.1 Wright’s $F_{ST}$ for seed banks and structured populations

Wright’s  $F_{ST}$  [Wri51] is a prominent but crude measure for population structure. There are various (more-or-less equivalent) formulations of this quantity in the literature. Here, we follow the notation and interpretation of Herbots [Her94, p. 73], which extensively studies this quantity for various structured multiple-island models. Indeed, define

$$F_{ST} := \frac{p_0 - \bar{p}}{1 - \bar{p}}, \quad (2)$$

where  $\bar{p}$  is the probability of *identity* of two genes sampled uniformly at random from the whole population, while  $p_0$  is the probability of identity of two genes sampled uniformly from a single sub-population, itself previously randomly sampled with probability given by its relative population size.

In the two-alleles model, the quantities  $\bar{p}$  and  $p_0$  will be given by the sample homozygosity (or, equivalently, the sample heterozygosity), whereas in the IAM and the ISM (cf. 1.3), we will argue in terms of the notion of *identity by descent*. Note that values of  $F_{ST} > 0$  indicate the presence of population structure. Its exact interpretation is not easy and depends on the details of the biological scenario. Hartl and Clark ([HC97]) argue that  $F_{ST} \in (0.05, 0.15)$  constitutes “moderate” genetic differentiation. Here, we will be interested how the quantity compares on in an theoretical level between the seed bank and the two island scenario, where the latter certainly represents a strongly structured population.

We begin with the derivation of  $F_{ST}$  in the two-alleles model.

**Sample heterozygosity in the two alleles model** The *sample heterozygosity*  $H$  of a population is defined to be the probability of finding two different alleles in a sample of size two drawn independently and uniformly from the population. In  $\mathsf{K}$  and  $\mathsf{W}$  the sample heterozygosity at stationarity is given by

$$H^{\mathsf{K}} := 2\mathbb{E}^{\mathsf{K}}[X(1-X)], \quad \text{and} \quad H^{\mathsf{W}} := 2\mathbb{E}^{\mathsf{W}}[X(1-X)],$$

where  $X$  has the stationary distribution of the diffusion corresponding to each model as given in (1).

A well-known result found e.g. in [Eth11, p. 49] states that

$$H^{\mathsf{K}} = \frac{4u_1u_2}{(u_1 + u_2)(1 + 2u_1 + 2u_2)}.$$

In a similar way, we can prove that the sample heterozygosity at stationarity under ( $\mathsf{W}$ ) is very similar to the one under ( $\mathsf{K}$ ) (which makes sense since the corresponding diffusions differ only in the coefficient of the noise term):

$$H^{\mathsf{W}} = \frac{4u_1u_2}{(u_1 + u_2)(\beta^2 + 2u_1 + 2u_2)}.$$

In the presence of population structure, e.g. in the form of a seed bank or separate islands, one distinguishes between the *global* resp. the individual *local* sample heterozygosities, corresponding to samples taken from the total population, resp. from each sub-population. Thus, with  $(X, Y)$  being the solution to (1) at stationarity, the local sample heterozygosities for each sub-population under  $\mathsf{S}$  and  $\mathsf{TI}$  are

$$\begin{aligned} H_X^{\mathsf{S}} &:= 2\mathbb{E}^{\mathsf{S}}[X(1-X)], & H_X^{\mathsf{TI}} &:= 2\mathbb{E}^{\mathsf{TI}}[X(1-X)], \\ H_Y^{\mathsf{S}} &:= 2\mathbb{E}^{\mathsf{S}}[Y(1-Y)], & H_Y^{\mathsf{TI}} &:= 2\mathbb{E}^{\mathsf{TI}}[Y(1-Y)], \end{aligned}$$

and therefore the global sample heterozygosities can be written as

$$\begin{aligned} H^{\mathsf{S}} &:= \frac{2K^2}{(K+1)^2} H_X^{\mathsf{S}} + \frac{2K}{(K+1)^2} \mathbb{E}_{\mu^{\mathsf{S}}}[X(1-Y) + Y(1-X)] + \frac{2}{(K+1)^2} H_Y^{\mathsf{S}}, \\ H^{\mathsf{TI}} &:= \frac{2K^2}{(K+1)^2} H_X^{\mathsf{TI}} + \frac{2K}{(K+1)^2} \mathbb{E}_{\mu^{\mathsf{TI}}}[X(1-Y) + Y(1-X)] + \frac{2}{(K+1)^2} H_Y^{\mathsf{TI}}. \end{aligned} \quad (3)$$

While the sample heterozygosity at stationarity (in the two-allele model) is well-studied for the Wright-Fisher and the two-island model (see e.g. [Her94], where the author also considers more complex multiple-island models), it has so far not been considered for seed banks.

Note that we can rewrite the sample heterozygosities for  $\mathsf{I} \in \{\mathsf{S}, \mathsf{TI}\}$  in terms of mixed moments using the notation

$$M_{n,m}^{\mathsf{I}} := \mathbb{E}_{\mu^{\mathsf{I}}}[X^n Y^m], \quad n, m \geq 0.$$

This immediately gives

$$H_X^{\mathsf{I}} = 2(M_{1,0}^{\mathsf{I}} - M_{2,0}^{\mathsf{I}}), \quad H_Y^{\mathsf{I}} = 2(M_{0,1}^{\mathsf{I}} - M_{0,2}^{\mathsf{I}}),$$

and therefore

$$H^{\text{I}} = \frac{2}{(K+1)^2} \left( (K^2 + K)M_{1,0}^{\text{I}} + (K+1)M_{0,1}^{\text{I}} - 2KM_{1,1}^{\text{I}} - K^2M_{2,0}^{\text{I}} - M_{0,2}^{\text{I}} \right).$$

From [BBGW19, Lemma 2.7] it is known that these mixed moments can be calculated recursively. For example, we obtain  $M_{0,0}^{\text{I}} = 1$  and

$$M_{1,0}^{\text{I}} = \frac{cu'_2 + u_1u'_2 + u_2u'_2 + cKu_2}{cu'_1 + cu'_2 + u_1u'_1 + u_1u'_2 + u_2u'_1 + u_2u'_2 + cKu_1 + cKu_2},$$

$$M_{0,1}^{\text{I}} = \frac{cu'_2 + u'_1u_2 + u_2u'_2 + cKu_2}{cu'_1 + cu'_2 + u_1u'_1 + u_1u'_2 + u_2u'_1 + u_2u'_2 + cKu_1 + cKu_2},$$

for the first moments, which interestingly do not explicitly depend on  $\alpha$  and  $\alpha'$ . Hence these values coincide for the two-island and the seed bank model. The expression for the second moments are much more complex and omitted for brevity, but can be computed easily.

For example, in the case of equal relative population sizes ( $K = 1$ ), migration rate  $c = 1$  and mutation rates  $u_1 = u_2 = u'_1 = u'_2 = 1/2$ , we obtain

$$H^{\text{S}} = \frac{14}{31} \approx 0.4516 > H^{\text{TI}} = \frac{13}{32} \approx 0.4063 > \frac{1}{3} = H^{\text{K}}.$$

Moreover, using simple sign arguments, we can fine out that these relationships also hold in a more general context: if  $u_1 = u'_1$  and  $u_2 = u'_2$ , then, for all  $u_1, u_2, c \geq 0$  and  $K = 1$ , we have  $H^{\text{S}} \geq H^{\text{TI}} \geq H^{\text{K}}$ . In particular, the sample heterozygosity in the Kingman case represents a lower bound.

However, in all other cases (e.g.  $c = u_1 = u_2 = u'_1 = u'_2 = 1$ ,  $K = 0.01$ ), the second inequality does not hold (if we violate either of the two conditions).

This indicates that a strong seed bank at stationarity retains elevated levels of genetic variability relative to a two island or panmictic model. The sample heterozygosity in the two-island case is somewhat lower, which is consistent with the idea that genetic drift (in the second island) reduces variability.

**Remark 2.1** (Scaling limit as second island / seed bank size approaches 0). Note that if we naively let  $K \rightarrow \infty$  (this corresponds to the relative second island / seed bank size  $\rightarrow 0$ ) in equation 3, ignoring the intrinsic dependence of the variables  $X$  and  $Y$  on this parameter, we recover the sample heterozygosity of the Kingman and weak seed bank case, i.e.

$$H_X^{\text{S}} \rightarrow H^{\text{K}} \quad \text{and} \quad H_X^{\text{TI}} \rightarrow H^{\text{K}}.$$

This aligns well with intuition. Indeed, this convergence holds in a much stronger sense on the diffusion level, and will be discussed theoretically in related future work.

**Remark 2.2** (Differentiating between scenarios K and W). The sample heterozygosity at stationarity cannot be used to distinguish between the Kingman case K and that of a weak seed bank W. But K and W can be differentiated using, for example, the *rate of*

decay of sample heterozygosity over time *in the absence of mutation*, i.e.  $u_1 = u_2 = 0$ , in which case the diffusion will eventually be absorbed in  $\{0, 1\}$ . Define

$$H^I(t, x) := 2\mathbb{E}^I[X(t)(1 - X(t)) | X(0) = x],$$

for  $I \in \{K, W\}$ , where the  $X(0) = x$  refers to the starting allele frequency in 1. Then we obtain

$$H^K(t, x) = 2e^{-t}x(1 - x), \quad \text{while} \quad H^W(t, x) = 2e^{-\beta^2 t}x(1 - x).$$

**Wright's  $F_{ST}$  for the two-alleles model.** In the previous section we derived the sample heterozygosities, i.e. the probabilities of sampling *distinct* types, in the two-alleles model. Of course, the probabilities of sampling *identical* types are simply their complement and thus we immediately obtain the identity

$$F_{ST}^I = \frac{(K + 1)H^I - KH_X^I - H_Y^I}{(K + 1)H^I}$$

for the strong seed bank  $I = S$  and the two-island model  $I = TI$ .

For example, fixing  $u_1 = u_2 = 1/2 = u'_1 = u'_2$ ,  $c = K = 1$  and  $\alpha = 1$ , the two-island model  $TI$  ( $\alpha' = 1$ ) leads to a stronger differentiation than the corresponding seed bank model  $S$  ( $\alpha' = 0$ ):

$$F_{ST}^S = \frac{1}{28} < \frac{1}{13} = F_{ST}^{TI}.$$

This indicates that strong seed banks indeed introduce some population substructure, but that the effect is stronger for the two island model. This is intuitively plausible, since both demes undergoing genetic drift leads to behavior that is closer to two independent populations than when genetic drift only takes place in one deme.

To further analyze how  $F_{ST}$  depends on the model parameters in both cases we refer to Figure 1. There, the first plot shows  $F_{ST}$  as a function of the migration rate  $c$ . As expected, the  $F_{ST}$  approaches 0 as  $c$  increases, leading to a well-mixed population, and the population structure in the two island model consistently dominates the one of the seed bank model by roughly a factor of approximately 2.1 (for this parameter choice). A similar result is visible in the second plot, where the  $F_{ST}$  is considered a function of the mutation rate. This is again in accordance to expectations, since increasing mutation rates while keeping them equal in both subpopulations also further mixes the populations. The third plot shows the dependence of  $F_{ST}$  on the relative population size  $K$ . Under both  $S$  and  $TI$ ,  $F_{ST}$  is nearly 0 if the relative population size on either island is very small (i.e.  $K$  either very small or very large), as this results in a correspondingly small probability of sampling two individuals from different demes when sampling uniformly among the whole population.

In the absence of mutation in the seed bank,  $u' = 0$ , and with our usual parameter choices  $u_1 = u_2 = 1/2$ ,  $K = c = 1$ , we get

$$F_{ST}^S = \frac{1}{27} > \frac{1}{28},$$

a *slightly* stronger signal than in the case with mutation. The relationship between  $K$ ,  $c$  and the  $F_{ST}$  in this setting is further illustrated in Figure 1.

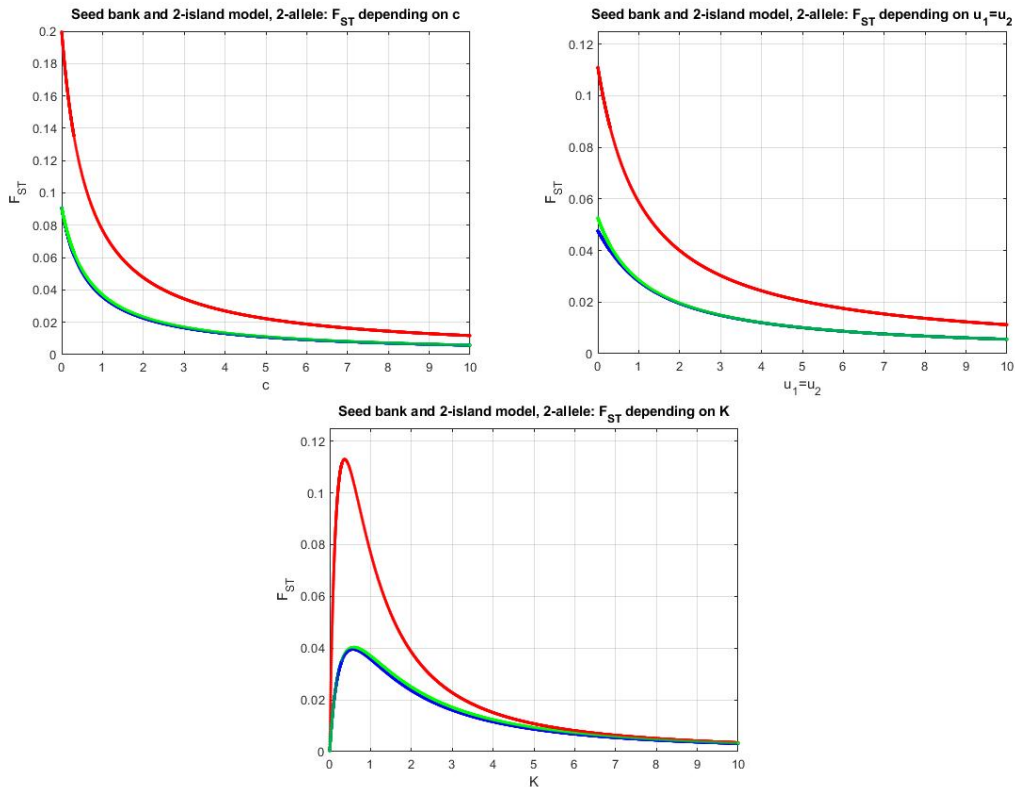


Figure 1:  $F_{ST}$  under the two island (red,  $u_1 = u_2 = u'_1 = u'_2$ ) and strong seed bank models (green for  $u'_1 = u'_2 = 0$ , blue for  $u'_1 = u'_2 = u_1 = u_2$ ) as a function of various parameters in the two-allele model. Where not specified,  $K = c = 1$ ,  $u_1 = u_2 = 0.5$ .

**Wright's  $F_{ST}$  for the infinite alleles model.** In contrast to the finite-alleles model, in the infinite alleles model every mutation leads to an entirely new allele. Hence, two sampled types are identical if and only if neither of their ancestral lineages mutated since the time of their most recent ancestor. Thus  $p_0$  and  $\bar{p}$  from (2) can be expressed as the so-called probabilities of *identity by descent* (IBD), and these probabilities can easily be represented in terms of the coalescent of the corresponding model K, W, S, TI.

Let  $T$  be the (random) *time to the most recent common ancestor* (TMRCA) of a sample of size 2 in any of the above coalescent models and observe that, if we assume the same mutation rate  $u = u'$  in both sub-populations (for S, TI), the probability that we do not see any mutations along the branches of the coalescent up to a time  $t > 0$  is given by  $e^{-u2t}$ . Since mutations in the IAM arise conditionally independently given  $T$  we have

$$p_0 = \mathbb{E}_{\pi_0}[e^{-2uT}] \quad \text{and} \quad \bar{p} = \mathbb{E}_{\bar{\pi}}[e^{-2uT}],$$

where  $\mathbb{E}_{\pi_0}$  is the expectation when the both genes are sampled from the same population, itself previously sampled among all populations according to its relative size, and similarly  $\mathbb{E}_{\bar{\pi}}$  is the expectation when the genes are sampled uniformly from the whole population. Note that the probability of identity by descent has recently been

investigated for  $\mathbf{S}$  in [dHP17] in the case of a finite population with seed bank on a discrete torus.

More generally, to obtain an expression for the quantities for possibly distinct mutation rates  $u \neq u'$ , we need to trace the time the lineages spend in each population before the TMRCA. To this end, let  $R_{2,0}$ ,  $R_{1,1}$  and  $R_{0,2}$  be the time until coalescence the ancestral lineages of a sample of 2 spend both in the first population, one lineage in each population and both in the second population, respectively. Then  $T = R_{2,0} + R_{1,1} + R_{0,2}$  and we get

$$p_0 = \mathbb{E}_{\pi_0} \left[ e^{-2uR_{2,0} - (u+u')R_{1,1} - 2u'R_{0,2}} \right] \quad \text{and} \quad \bar{p} = \mathbb{E}_{\bar{\pi}} \left[ e^{-2uR_{2,0} - (u+u')R_{1,1} - 2u'R_{0,2}} \right].$$

Phase-type distribution theory [HSJB18] yields elegant closed form expressions for these quantities.

**Proposition 2.3.** *Assuming the IAM, the fixation index  $F_{ST}^I$  for  $I \in \{\mathbf{S}, \mathbf{TI}\}$  is given by*

$$F_{ST}^I = \frac{p_0^I - \bar{p}^I}{1 - \bar{p}^I}$$

where

$$p_0^I = \pi_0(A - S^I)^{-1} s^I \quad \text{and} \quad \bar{p}^I = \bar{\pi}(A - S^I)^{-1} s^I$$

for

$$\pi_0 := \left( \frac{K}{1+K}, 0, \frac{1}{1+K} \right), \quad \bar{\pi} := \left( \frac{K^2}{(1+K)^2}, \frac{2K}{(1+K)^2}, \frac{1}{1+K} \right)$$

and

$$A = \begin{bmatrix} -2u & 0 & 0 \\ 0 & -(u+u') & 0 \\ 0 & 0 & -2u' \end{bmatrix}.$$

One sets

$$S^{\mathbf{TI}} = \begin{bmatrix} -(2c+1) & 2c & 0 \\ cK & -(cK+c) & c \\ 0 & 2cK & -(2cK+1/K) \end{bmatrix} \quad \text{and} \quad s^{\mathbf{TI}} = \begin{bmatrix} 1 \\ 0 \\ 1/K \end{bmatrix}$$

for the two-island model  $\mathbf{TI}$ , and

$$S^{\mathbf{S}} = \begin{bmatrix} -(2c+1) & 2c & 0 \\ cK & -(cK+c) & c \\ 0 & 2cK & -2cK \end{bmatrix} \quad \text{and} \quad s^{\mathbf{S}} = \begin{bmatrix} 1 \\ 0 \\ 0 \end{bmatrix}$$

for the strong seed bank model  $\mathbf{S}$ .

The proof is obtained using the machinery of [HSJB18] and we adhere to the notation used therein for the convenience of the reader. Example 2.4 in [HSJB18] calculates different functionals of the seed bank coalescent, as the expected TMRCA and tree-lengths, but not the quantities considered here.

*Proof.* Let  $Z$  be a time-continuous Markov chain on the finite space

$$E := \{(2, 0), (1, 1), (0, 2), (*, *)\}$$

with Q-matrix

$$Q^{\mathbb{I}} = \begin{bmatrix} S^{\mathbb{I}} & s^{\mathbb{I}} \\ 0 & 0 \end{bmatrix} \quad \text{where } S^{\mathbb{I}} = \begin{bmatrix} -(2c+1) & 2c & 0 \\ cK & -(cK+c) & c \\ 0 & 2cK & -(2cK+\alpha^{\mathbb{I}}) \end{bmatrix}$$

$$\text{and } s^{\mathbb{I}} = \begin{bmatrix} 1 \\ 0 \\ \alpha^{\mathbb{I}} \end{bmatrix}$$

for  $\alpha^{\mathbb{I}} = 1/K$  if  $\mathbb{I} = \text{TI}$  and 0 otherwise. Note that  $Z$  traces whether the lineages of a sample of 2 are both in the first population, one in each population or both in the second population for the two-island and the seed bank model depending on the choice of  $\alpha^{\mathbb{I}}$ . The state  $(*, *)$  is reached precisely at the time of coalescence, i.e. at the TMRCA  $T$  of the sample of 2, and is the only absorbing state. Recall that  $R_{2,0}$  was the time the ancestral lineages of the sample spent both in the first population and note that we can write it as

$$R_{2,0} = \int_0^T r_{2,0}(Z_t) dt$$

for a function  $r_{2,0} : B \rightarrow \mathbb{R}$  with  $r_{2,0}((2,0)) = 1$  and equal to 0 otherwise. We can do the same for  $R_{1,1}$  and  $R_{0,2}$  with analogous functions and thus Theorem 2.5 in [HSJB18] immediately yield

$$p_0 = \mathbb{E}_{\pi_0} \left[ e^{-2uR_{2,0} - (u+u')R_{1,1} - 2u'R_{0,2}} \right]$$

$$= \pi_0 \left( \left( \begin{bmatrix} -2u & 0 & 0 \\ 0 & -(u+u') & 0 \\ 0 & 0 & -2u' \end{bmatrix} - S^{\mathbb{I}} \right)^{-1} s^{\mathbb{I}} \right)$$

and analogously for  $\bar{p}$ . □

Figure 2 illustrates the  $F_{ST}$  under different choices of parameters for the infinitely many allele case. As we can see, the pictures differ from those in the 2-allele case only slightly.

**Wright's  $F_{ST}$  for the infinite sites model.** The central difference between the IAM and the ISM is that all previous mutations on a lineage remain observable in the latter. However, this does not affect the probability of identity by descent of two sampled individuals — they will still carry the same allele if and only if neither ancestral line mutated during the time from their MRCA to the present. Thus, sample heterozygosity  $H$  and  $F_{ST}$  under the ISM can be computed in exactly the same way as in the IAM and we refer to the previous section for the explicit formulas.

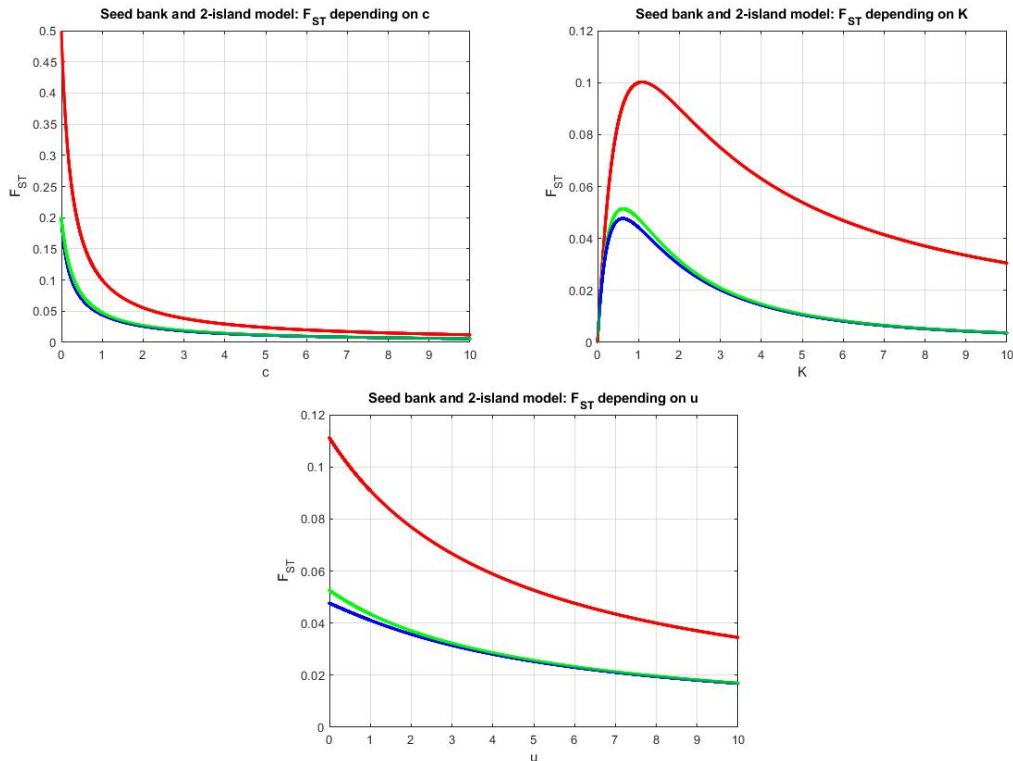


Figure 2:  $F_{ST}$  under the two island (red,  $u = u'$ ) and strong seed bank models (green for  $u' = 0$ , blue for  $u' = u$ ) as a function of various parameters in the infinitely many allele model. Where not specified,  $K = c = 1$ ,  $u = 0.5$ .

## 2.2 The site frequency spectrum (SFS) in the ISM

Since information about the past mutation history of lineages is retained in the ISM, one may want to consider more informative summary statistics. One of the most frequently used examples is the *site frequency spectrum* (SFS). For a sample of size  $k$  it is given by a vector  $(\zeta_1^{(k)}, \dots, \zeta_{k-1}^{(k)})$ , with  $\zeta_i^{(k)}$  denoting the number of sites at which the *derived* allele, i.e. a mutation, is observed  $i$  times in the sample. This assumes that we know the wildtype and are therefore able to determine which of the possibly two occurring alleles is the result of a mutation and which is the original. In the case where we do not know which allele is ancestral and which is derived, the *folded site frequency spectrum*  $(\eta_1^{(k)}, \dots, \eta_{\lfloor k/2 \rfloor}^{(k)})$  can be used instead, where  $\eta_i^{(k)}$  is the number of sites where two variants of an allele are observed with multiplicities  $i : k - i$ .

The SFS is well understood for the classical Kingman coalescent  $\mathbb{K}$ , and thus also in the case  $\mathbb{W}$ , since the weak seed bank coalescent is just a constant time-change of the Kingman [ZT12, Formula 1].

We can also calculate the *expected* SFS for the cases  $\mathbb{TI}$  and  $\mathbb{S}$ . We consider  $k$  individuals sampled according to some initial distribution  $\pi$  from the first and the second population. Since the mutations in the ISM are assumed to occur according to a Poisson process conditionally on the coalescent,  $\mathbb{E}^\pi[\zeta_i^{(k)}]$  is the product of the mutation

rate and the total lengths of branches that are ancestral to  $i$  individuals, for which phase-type distribution theory is well suited. In order to state the result (and thereby give the bulk of the proof), we require a few technical definitions, but the calculation of the SFS then reduces to a simple vector-matrix multiplication in Proposition 2.4. The structure is reminiscent of the observations for the SFS of  $\Lambda$ -coalescents in [HSJB18].

As in Proposition 2.3 we want to define an auxiliary Markov chain. Its state space  $E$  should be small to minimize computational cost, but needs to be sufficiently large to contain all information necessary to calculate the SFS. More precisely, we need to know how many lineages are ancestral to  $i$  individuals in the sample at any time in the coalescent and we need to know which of these lineages are in the first and which are in the second population in order to account for different mutation rates. For a sample of size  $k$  define

$$E := \left\{ \{0, \dots, k\}^{2k} \mid \sum_{i=1}^k i(a_i + a_{k+i}) = k \right\} \setminus \{e_k, e_{2k}\}$$

where  $e_k$  and  $e_{2k}$  are the vectors with the entry 1 in positions  $k$  and  $2k$  respectively (and thus 0 everywhere else). We remove these in order to identify them as what will be the unique absorbing state of the Markov chain. Thus define

$$E^* := E \cup \{*\}.$$

For  $a \in E$ , if  $i = 1, \dots, k$ , the quantity  $a_i$  is the number of lineages currently in the first population that are ancestral to  $i$  of the sampled individuals (independently of their origin). If  $i = k + 1, \dots, 2k$  then  $a_i$  is the analogous number of lineages in the second population.

Given this interpretation, it becomes easy to identify the set  $E_0$  of sensible starting points for the auxiliary Markov chain:

$$E_0 := \{a \in E \mid a_k + a_{2k} = k\}.$$

The auxiliary Markov chain starting in such an  $a \in E_0$  corresponds to a sample of  $a_k$  individuals from the first and  $a_{2k}$  individuals from the second population. Let  $\pi$  be a distribution on  $E^*$ , concentrated on  $E_0$ . i.e. such that  $\sum_{a \in E_0} \pi(a) = 1$ . This will be the initial distribution of the Markov chain.

The only allowed transitions of the chain will be those corresponding to a coalescence (possibly in both populations) or that of a migration. For  $z \in \mathbb{Z}$  let  $(z)^+ := \max\{z, 0\}$  and  $(z)^- := \min\{z, 0\}$ . Let  $a, b \in E$ . We call a transition from the state  $a$  to the state  $b$  a *coalescence*, if

- (i)  $\sum_{j=1}^{2k} (b_j - a_j)^- = -2$ ,
- (ii)  $\sum_{j=1}^{2k} (b_j - a_j)^+ = 1$ ,
- (iii)  $\sum_{j=1}^k j(b_j - a_j) = 0$ .

The first two sums describe the effect of the coalescence of two lineages. Note that the last sum only runs until  $k$ , thereby ensuring that the coalescence takes place between lineages of the same population. A transition from  $a$  to  $b$  will be called a *migration*, if on the other hand

- (i)  $\sum_{j=1}^{2k} (b_j - a_j)^- = -1$ ,
- (ii)  $\sum_{j=1}^{2k} (b_j - a_j)^+ = 1$ .

The rates at which the Markov chain then transitions between the states  $a, b \in E$ , of course, depend on the model considered and are then given by

$$S_{a,b}^{\mathbb{I}} := c \sum_{j=1: b_j - a_j < 0}^k a_j + cK \sum_{j=1: b_{k+j} - a_{k+j} < 0}^k a_{k+j},$$

if  $a \mapsto b$  is a *migration* and

$$S_{a,b}^{\mathbb{I}} := \prod_{j=1: b_j - a_j < 0}^k \binom{a_j}{b_j - a_j} + \alpha \prod_{j=1: b_{k+j} - a_{k+j} < 0}^k \binom{a_{k+j}}{b_{k+j} - a_{k+j}},$$

if it is a *coalescence*, where we set  $\alpha = 0$  if  $\mathbb{I} = \mathbb{S}$  and  $\alpha = 1/K$ , if  $\mathbb{I} = \mathbb{TI}$ . For any other  $a \neq b$  set  $S_{a,b}^{\mathbb{I}} := 0$ .

Next, define  $s^{\mathbb{I}} : E \rightarrow [0, \infty[$

$$s^{\mathbb{I}}(a) := \begin{cases} 1, & \text{if } \sum_{j=1}^{2k} a_j = \sum_{j=1}^k a_j = 2, \\ \alpha, & \text{if } \sum_{j=1}^{2k} a_j = \sum_{j=k+1}^{2k} a_j = 2, \\ 0, & \text{otherwise,} \end{cases}$$

where we choose  $\alpha = 1/K$  for  $\mathbb{I} = \mathbb{TI}$  and  $\alpha = 0$  for  $\mathbb{I} = \mathbb{S}$ . Note that  $s^{\mathbb{I}}$  is non-zero precisely on the states describing the respective coalescents having two lineages left which might coalesce and gives the corresponding rates of this event.

With this now define the matrix  $S^{\mathbb{I}} = (S_{a,b}^{\mathbb{I}})_{a,b \in E}$  through

$$S_{a,b}^{\mathbb{I}} := \begin{cases} S_{a,b}, & \text{if } a \neq b, \\ -(\sum_{a' \in E} S_{a,a'} + s^{\mathbb{I}}(a)) & \text{if } a = b. \end{cases}$$

Finally, we define for any  $i = 1, \dots, k-1$ :  $r_i(\ast) := 0$  and for every  $a \in E$

$$r_i(a) := ua_i + u'a_{k+i}.$$

Note that, if you sort the elements of  $E^*$ , for example in lexicographical order,  $\pi, r_1, \dots, r_{k-1}$  are normal vectors and  $S^{\mathbb{I}}$  is a matrix, hence the following result should be read as a vector-matrix multiplication.

**Proposition 2.4.** *Assume the ISM, with mutation rates  $u, u' \geq 0$  in the first and second population, respectively. Furthermore, let  $\pi$  describe how the  $k \in \mathbb{N}$  individuals are sampled from the first and second population. With the notation introduced above, we have*

$$\mathbb{E}^\pi \left[ \zeta_i^{(k)} \right] = \pi(-S^{\mathbf{I}})^{-1} r_i \quad (4)$$

for all  $i = 1, \dots, k-1$  and  $\mathbf{I} \in \{\mathbf{TI}, \mathbf{S}\}$ .

Indeed, for a sample of  $k_1$  individuals from the first population and  $k_2 = k - k_1$  individuals from the second population, use  $\pi^{(k_1, k_2)} : E^* \rightarrow [0, 1]$  defined as

$$\pi^{(k_1, k_2)}(a) := \begin{cases} 1, & \text{if } a_1 = k_1 \text{ and } a_{k+1} = k_2, \\ 0, & \text{otherwise.} \end{cases}$$

For a sample drawn uniformly among the whole populations, taking into consideration the relative population size  $K$ , one chooses  $\pi^{\text{unif}} : E^* \rightarrow [0, 1]$  defined as

$$\pi^{\text{unif}}(a) := \begin{cases} \frac{1}{K+1} \binom{k}{a_{2k}} K^{a_{2k}}, & \text{if } a \in E_0, \\ 0, & \text{otherwise.} \end{cases}$$

Note that equation (8) in [HSJB18] indeed gives an expression for all mixed moments of the SFS  $(\zeta_1^{(k)}, \dots, \zeta_{k-1}^{(k)})$  using the quantities defined above.

*Proof.* Let  $Z$  be a (time-continuous) Markov chain with state space  $E^*$  and (conservative) Q-matrix

$$Q := \begin{bmatrix} S^{\mathbf{I}} & s^{\mathbf{I}} \\ 0 & 0 \end{bmatrix}.$$

Started in  $\pi$ , the time to absorption  $\tau$  of  $Z$  in  $*$  is equal to the time to the most recent common ancestor in  $\mathbf{I}$ , if the sample of  $k$  is drawn according to  $\pi|_{E_0}$ , with the obvious correspondence between the two state-spaces. (This holds in distribution, but the processes can obviously be coupled for this to be true even pathwise.) Since the mutations occur independently of the coalescent, to compute  $\mathbb{E}^\pi[\zeta_i^{(k)}]$ , we simply trace the time a lineage in the coalescent is ancestral to  $i$  of the initial individuals and multiply it by  $u$  when it is in the first and by  $u'$  when it is in the second population. This is precisely what is done by the reward functions  $r_1, \dots, r_{k-1}$ . More precisely, if we define

$$\tilde{\zeta}_i^{(k)} := \int_0^\tau r_i(Z_t) dt,$$

then

$$\mathbb{E}^\pi \left[ \zeta_i^{(k)} \right] = \mathbb{E}^\pi \left[ \tilde{\zeta}_i^{(k)} \right]$$

and therefore equation (8) in [HSJB18] yields equation (4) above.  $\square$

**Remark 2.5.** Similarly, one might be interested in the normalized expected site frequency spectrum (NESFS)  $(E\hat{\zeta}_1^{(k)}, \dots, E\hat{\zeta}_{k-1}^{(k)})$ , as introduced in [EBBF15, p. 13]. It is defined by

$$E\hat{\zeta}_i^{(k)} := \frac{\mathbb{E}[\zeta_i^{(k)}]}{\sum_{l=2}^k l\mathbb{E}[T_l]},$$

$T_l$  being the time up to the time to the most recent common ancestor during which there are  $l$  distinct lineages present in the coalescent (regardless of what population they might belong to),  $l = 2, 3, \dots, n$ . In other words,  $\sum_{l=2}^k l\mathbb{E}[T_l]$  is the average tree length. Its interest comes from the fact that the NESFS is a first-order approximation of the expectation of the normalized SFS, given by

$$\hat{\zeta}_i^{(k)} := \frac{\zeta_i^{(k)}}{\zeta_1^{(k)} + \dots + \zeta_{k-1}^{(k)}},$$

cf. [EBBF15, p. 9]. The distribution of  $(\hat{\zeta}_1^{(k)}, \dots, \hat{\zeta}_{k-1}^{(k)})$  is very insensitive to the mutation rate, provided the latter is not too small, facilitating practical inference when the mutation rate is unknown [EBBF15, Supporting Information, pages SI12 – SI13]. Note that, the average tree length for the seed bank model **S** was analyzed in [HSJB18] and thus all necessary quantities to calculate the normalized expected SFS are given.

Figures 3 and 4 provide illustrations of the expected SFS, with and without normalization.

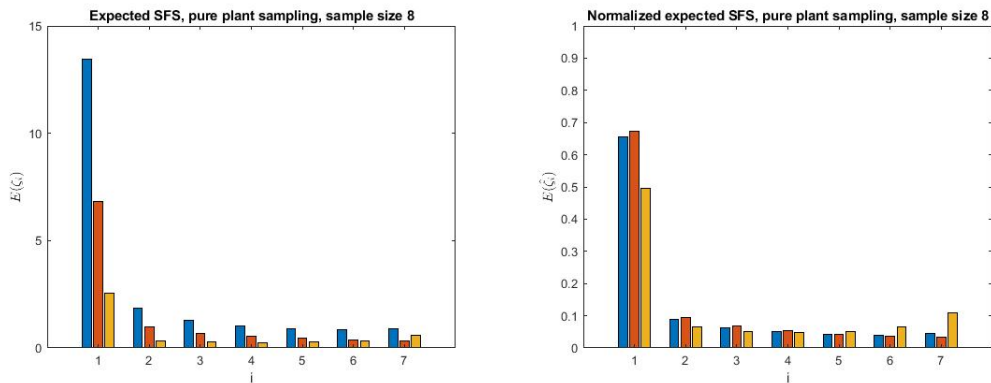


Figure 3: Expected SFS for a sample of size  $k = 8$  chosen purely from the active population, i.e.  $\pi^{(8,0)}$ .  $K = c = u = 1$ . Blue corresponds to **S**, orange to **TI**, with  $\alpha = \alpha' = 1$ , and yellow to **K** for comparison.

It is noteworthy that the magnitude of entries in the (expected) SFS varies strongly between the three models, while **S** and **TI** have very similar normalized spectra. The implication is that all three models are straightforward to tell apart if the population-rescaled mutation rate is known, but that a larger sample, or a more informative summary statistic, is needed to distinguish **S** from **TI** when it is unknown.

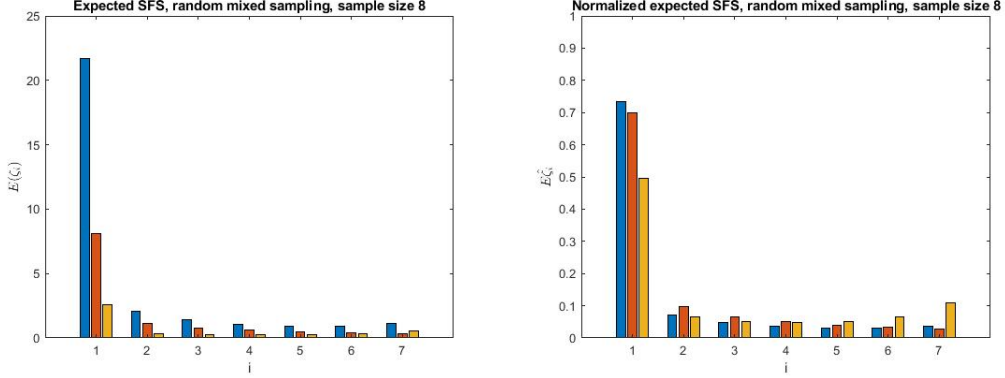


Figure 4: Expected SFS for a sample of size  $k = 8$  chosen uniformly from the whole population, i.e.  $\pi^{\text{unif}}$ .  $K = c = u = 1$ . Blue corresponds to **S**, orange to **TI**, with  $\alpha = \alpha' = 1$ , and yellow to **K** for comparison. Expected SFS when sampling uniformly from the total population.

### 3 Recursions for the sampling distributions

In this section we use recursions to characterize the (in general intractable) sampling distributions for scenario **S**, and all three classes of mutation models (**IAM**, **FAM**, and **ISM**). The corresponding recursions for scenarios **K**, **W**, and **TI** are well-known, and special cases of [DG04, equation (2)]. We will also describe a low-variance Monte Carlo scheme to approximate solutions of these recursions, and hence conduct unbiased inference and model selection based on full likelihoods.

#### 3.1 IAM recursion

Let  $p(\mathbf{n}^{(1)}; \mathbf{n}^{(2)})$  be the probability of observing sample  $\mathbf{n}^{(1)}$  from the active population, and  $\mathbf{n}^{(2)}$  from the seed bank under scenario **S**, and  $\mathbf{e}_i$  be the canonical unit vector with a 1 in the  $i$ th place, and zeros elsewhere. Then  $p(\mathbf{n}^{(1)}; \mathbf{n}^{(2)})$  solves

$$\begin{aligned}
& \left[ n^{(1)} \left( \frac{n^{(1)} - 1}{2} + u + c \right) + n^{(2)}(u' + Kc) \right] p(\mathbf{n}^{(1)}; \mathbf{n}^{(2)}) \\
&= un^{(1)} \sum_{i: (n_i^{(1)}, n_i^{(2)}) = (1, 0)} p(\mathbf{n}^{(1)} - \mathbf{e}_i; \mathbf{n}^{(2)}) + u'n^{(2)} \sum_{i: (n_i^{(1)}, n_i^{(2)}) = (0, 1)} p(\mathbf{n}^{(1)}; \mathbf{n}^{(2)} - \mathbf{e}_i) \\
&+ \frac{n^{(1)}}{2} \sum_{i: n_i^{(1)} \geq 2} (n_i^{(1)} - 1) p(\mathbf{n}^{(1)} - \mathbf{e}_i; \mathbf{n}^{(2)}) \\
&+ cn^{(1)} \sum_{i: n_i^{(1)} \geq 1} \frac{n_i^{(2)} + 1}{n^{(2)} + 1} p(\mathbf{n}^{(1)} - \mathbf{e}_i; \mathbf{n}^{(2)} + \mathbf{e}_i) \\
&+ Kcn^{(2)} \sum_{i: n_i^{(2)} \geq 1} \frac{n_i^{(1)} + 1}{n^{(1)} + 1} p(\mathbf{n}^{(1)} + \mathbf{e}_i; \mathbf{n}^{(2)} - \mathbf{e}_i),
\end{aligned}$$

with boundary condition  $p(\mathbf{e}_i; 0) = p(0; \mathbf{e}_i) = 1$ . This recursion can be obtained from [DG04, equation (2)] by omitting those transitions which are not allowed in  $\mathbf{S}$ , and adjusting the coefficient on the left hand side accordingly.

### 3.2 FAM recursion

Under scenario  $\mathbf{S}$ , and the FAM, the sampling distribution  $p(\mathbf{n}^{(1)}; \mathbf{n}^{(2)})$  solves

$$\begin{aligned}
& \left[ n^{(1)} \left( \frac{n^{(1)} - 1}{2} + u_1 + u_2 + c \right) + n^{(2)}(u'_1 + u'_2 + Kc) \right] p(\mathbf{n}^{(1)}; \mathbf{n}^{(2)}) \\
&= u_2(n_1^{(1)} + 1)\mathbf{1}(n_2^{(1)} > 0)p(\mathbf{n}^{(1)} + \mathbf{e}_1 - \mathbf{e}_2; \mathbf{n}^{(2)}) \\
&\quad + u_1(n_2^{(1)} + 1)\mathbf{1}(n_1^{(1)} > 0)p(\mathbf{n}^{(1)} - \mathbf{e}_1 + \mathbf{e}_2; \mathbf{n}^{(2)}) \\
&\quad + u'_2(n_1^{(2)} + 1)\mathbf{1}(n_2^{(2)} > 0)p(\mathbf{n}^{(1)}; \mathbf{n}^{(2)} + \mathbf{e}_1 - \mathbf{e}_2) \\
&\quad + u'_1(n_2^{(2)} + 1)\mathbf{1}(n_1^{(2)} > 0)p(\mathbf{n}^{(1)}; \mathbf{n}^{(2)} - \mathbf{e}_1 + \mathbf{e}_2) \\
&\quad + n^{(1)}\frac{n_1^{(1)} - 1}{2}p(\mathbf{n}^{(1)} - \mathbf{e}_1; \mathbf{n}^{(2)}) + n^{(1)}\frac{n_2^{(1)} - 1}{2}p(\mathbf{n}^{(1)} - \mathbf{e}_2; \mathbf{n}^{(2)}) \\
&\quad + cn^{(1)}\frac{n_1^{(2)} + 1}{n^{(2)} + 1}\mathbf{1}(n_1^{(1)} > 0)p(\mathbf{n}^{(1)} - \mathbf{e}_1; \mathbf{n}^{(2)} + \mathbf{e}_1) \\
&\quad + cn^{(1)}\frac{n_2^{(2)} + 1}{n^{(2)} + 1}\mathbf{1}(n_2^{(1)} > 0)p(\mathbf{n}^{(1)} - \mathbf{e}_2; \mathbf{n}^{(2)} + \mathbf{e}_2) \\
&\quad + Kcn^{(2)}\frac{n_1^{(1)} + 1}{n^{(1)} + 1}\mathbf{1}(n_1^{(2)} > 0)p(\mathbf{n}^{(1)} + \mathbf{e}_1; \mathbf{n}^{(2)} - \mathbf{e}_1) \\
&\quad + Kcn^{(2)}\frac{n_2^{(1)} + 1}{n^{(1)} + 1}\mathbf{1}(n_2^{(2)} > 0)p(\mathbf{n}^{(1)} + \mathbf{e}_2; \mathbf{n}^{(2)} - \mathbf{e}_2),
\end{aligned}$$

where  $\mathbf{1}(E) = 1$  if event  $E$  is true, and 0 otherwise. Boundary conditions are typically prescribed as the stationary distribution specified by the mutation rates, at least when  $u_1 = u'_1$  and  $u_2 = u'_2$ :

$$\begin{aligned}
p((1, 0); (0, 0)) &= p((0, 0); (1, 0)) = \rho_1, \\
p((0, 1); (0, 0)) &= p((0, 0); (0, 1)) = \rho_2.
\end{aligned}$$

### 3.3 ISM recursion

The  $\mathbf{S}$  sampling recursion under the ISM is

$$\begin{aligned}
& \left[ n^{(1)} \left( \frac{n^{(1)} - 1}{2} + u + c \right) + n^{(2)}(u' + Kc) \right] p(\mathbf{t}, \mathbf{n}^{(1)}, \mathbf{n}^{(2)}) \\
&= u \sum_{\substack{i: n_i^{(1)}=1, n_i^{(2)}=0 \\ s_1^{(k)}(t_i) \neq t_j \forall j \forall k}} p(s_i^{(k)}(\mathbf{t}), \mathbf{n}^{(1)}, \mathbf{n}^{(2)}) + u' \sum_{\substack{i: n_i^{(1)}=0, n_i^{(2)}=1 \\ s_1^{(k)}(t_i) \neq t_j \forall j \forall k}} p(s_i^{(k)}(\mathbf{t}), \mathbf{n}^{(1)}, \mathbf{n}^{(2)})
\end{aligned}$$

$$\begin{aligned}
& + u \sum_{i:(n_i^{(1)}, n_i^{(2)})=(1,0)} \sum_{(j,k):s_1^{(k)}(t_i)=t_j} (n_j^{(1)} + 1)p(r_i(\mathbf{t}), r_i(\mathbf{n}^{(1)} + \mathbf{e}_j), r_i(\mathbf{n}^{(2)})) \\
& + u' \sum_{i:(n_i^{(1)}, n_i^{(2)})=(0,1)} \sum_{(j,k):s_1^{(k)}(t_i)=t_j} (n_j^{(2)} + 1)p(r_i(\mathbf{t}), r_i(\mathbf{n}^{(1)}), r_i(\mathbf{n}^{(2)} + \mathbf{e}_j)) \\
& + n^{(1)} \sum_{i:n_i^{(1)} \geq 2} \frac{n_i^{(1)} - 1}{2} p(\mathbf{t}, \mathbf{n}^{(1)} - \mathbf{e}_i, \mathbf{n}^{(2)}) \\
& + cn^{(1)} \sum_{i:n_i^{(1)} \geq 1} \frac{n_i^{(2)} + 1}{n^{(2)} + 1} p(\mathbf{t}, \mathbf{n}^{(1)} - \mathbf{e}_i, \mathbf{n}^{(2)} + \mathbf{e}_i) \\
& + Kcn^{(2)} \sum_{i:n_i^{(2)} \geq 1} \frac{n_i^{(1)} + 1}{n^{(1)} + 1} p(\mathbf{t}, \mathbf{n}^{(1)} + \mathbf{e}_i, \mathbf{n}^{(2)} - \mathbf{e}_i),
\end{aligned}$$

with boundary condition  $p(\emptyset, (1), (0)) = p(\emptyset, (0), (1)) = 1$ , and where  $s_i^{(k)}(\mathbf{t})$  removes the  $k^{\text{th}}$  element of  $t_i$ , e.g.

$$s_1^{(2)}(\{(0, 2, 3\}, \{1\})\}) = (\{0, 3\}, \{1\}),$$

while  $r_i(\mathbf{t})$  removes  $t_i$  entirely, e.g.

$$r_1(\{(0, 2, 3\}, \{1\})\}) = (\{1\}).$$

### 3.4 A Monte Carlo scheme for solving sampling recursions

The K and W coalescents under either IAM or parent-independent FAM mutation are the only instances of the sampling recursions listed above that can be solved explicitly. Numerical schemes for solving the recursions directly also fail for moderate sample sizes because of combinatorial explosion of the number of equations. Hence, Monte Carlo schemes are used to approximate solutions in practice. One example of such a scheme is importance sampling, which we briefly introduce below.

Suppose  $\{H_k\}_{k=0}^K$  denotes the history of a sample  $\mathbf{n}$ , so that  $H_0 = \mathbf{n}$ ,  $H_K$  is the type of the most recent common ancestor, and  $H_{k+1}$  differs from  $H_k$  by one coalescence, mutation, or migration event. Then the likelihood of the sample can be written as

$$\begin{aligned}
p(\mathbf{n}) &= \sum_{H_0, \dots, H_K} p(\mathbf{n}|H_0, \dots, H_K) \mathbb{P}(H_0, \dots, H_K) \\
&= \sum_{H_0} \dots \sum_{H_K} p(\mathbf{n}|H_0, \dots, H_K) p(H_K) \prod_{k=1}^K \mathbb{P}(H_{k-1}|H_k). \tag{5}
\end{aligned}$$

In fact, all of the recursions presented above represent decompositions of this form, with  $p(\mathbf{n}|H_0, \dots, H_K) = \mathbb{1}(H_0 = \mathbf{n})$ , with the coefficients of the various recursions denoting the transition probabilities  $\mathbb{P}(H_{k-1}|H_k)$ , and with  $p(H_K)$  corresponding to the boundary conditions. A naive Monte Carlo scheme for approximating this sum is to sample a most recent common ancestor from the law  $p(H_K)$ , evolve the sample

stochastically until it reaches the desired size  $n + 1$  with probabilities given by the coefficients of the appropriate sampling recursion, and then evaluate the quantity of interest  $\mathbb{1}(H_0 = \mathbf{n})$ , where  $H_0$  is the final sample with size  $n$ .

However, likelihoods in genetics can be vanishingly small, which renders the number of such simulations required for accurate estimators infeasibly large. Instead, we introduce an importance sampling proposal distribution  $\mathbb{Q}(H_k|H_{k-1})$ , which acts in the opposite direction of time to  $\mathbb{P}(H_{k-1}|H_k)$ , i.e. from the observed leaves towards the most recent common ancestor, and rewrite the summation in (5) as

$$p(\mathbf{n}) = \sum_{H_0} \dots \sum_{H_K} p(H_K) \prod_{k=1}^K \frac{\mathbb{P}(H_{k-1}|H_k)}{\mathbb{Q}(H_k|H_{k-1})} \mathbb{Q}(H_k|H_{k-1}).$$

We will specify  $\mathbb{Q}$  in such a way that  $\mathbb{Q}(H_0 = \mathbf{n}) = 1$ , which is why the factor  $p(\mathbf{n}|H_0, \dots, H_K)$  no longer appears. This initial condition is then propagated back to the most recent common ancestor with yet-to-be-specified transition probabilities  $\mathbb{Q}(H_k|H_{k-1})$ , and once the most recent common ancestor is reached, we can again evaluate the modified quantity of interest

$$p(H_K) \prod_{k=1}^K \frac{\mathbb{P}(H_{k-1}|H_k)}{\mathbb{Q}(H_k|H_{k-1})}.$$

Under this scheme, every sample results in a positive contribution with certainty, which reduces the variance of estimators, and careful choices of  $\mathbb{Q}$  can reduce variance even further.

The zero-variance proposal distribution  $\mathbb{Q}$  under scenario K (and thus also W) was described in [SD00], and extended to TI in [DG04]. None of these proposal distributions can be implemented, but both articles also provide heuristic approximations to the corresponding optimal algorithms, which result in low variance in practice. In this section we present the analogous minimum variance importance sampler for scenario S under all three models of mutation, and describe corresponding, approximately optimal implementations.

We begin with the two-allele model, and let  $p_i(\mathbf{e}_j|\mathbf{n}^{(1)}, \mathbf{n}^{(2)})$  denote the probability that a further lineage sampled from island  $i \in \{1, 2\}$  (recall that we identify the active population as island 1, and the seed bank as island 2) carries type  $j \in \{1, 2\}$ , given observed type frequencies  $\mathbf{n}^{(1)}, \mathbf{n}^{(2)}$  from islands 1 and 2, respectively. These conditional sampling distributions are intractable, but as outlined above, approximating them will turn out to produce efficient algorithms.

Let

$$D(n^{(1)}, n^{(2)}) := n^{(1)} \left( \frac{n^{(1)} - 1}{2} + u + c \right) + n^{(2)}(u' + Kc).$$

A calculation similar to that of Theorem 1 in [SD00] identifies the zero-variance importance sampling proposal distribution for the two-allele model as

$$(\mathbf{n}^{(1)}, \mathbf{n}^{(2)}) \mapsto (\mathbf{n}^{(1)} - \mathbf{e}_i, \mathbf{n}^{(2)}) \text{ with prob. } \frac{n_i^{(1)}(n_i^{(1)} - 1)/2}{p_1(\mathbf{e}_i|\mathbf{n}^{(1)} - \mathbf{e}_i, \mathbf{n}^{(2)})D(n^{(1)}, n^{(2)})},$$

$$\begin{aligned}
(\mathbf{n}^{(1)}, \mathbf{n}^{(2)}) &\mapsto (\mathbf{n}^{(1)} - \mathbf{e}_i + \mathbf{e}_j, \mathbf{n}^{(2)}) \text{ with prob. } \frac{un_i^{(1)}p_1(\mathbf{e}_j|\mathbf{n}^{(1)} - \mathbf{e}_i, \mathbf{n}^{(2)})}{p_1(\mathbf{e}_i|\mathbf{n}^{(1)} - \mathbf{e}_i, \mathbf{n}^{(2)})D(n^{(1)}, n^{(2)})}, \\
(\mathbf{n}^{(1)}, \mathbf{n}^{(2)}) &\mapsto (\mathbf{n}^{(1)}, \mathbf{n}^{(2)} - \mathbf{e}_i + \mathbf{e}_j) \text{ with prob. } \frac{u'n_i^{(2)}p_2(\mathbf{e}_j|\mathbf{n}^{(1)}, \mathbf{n}^{(2)} - \mathbf{e}_i)}{p_2(\mathbf{e}_i|\mathbf{n}^{(1)}, \mathbf{n}^{(2)} - \mathbf{e}_i)D(n^{(1)}, n^{(2)})}, \\
(\mathbf{n}^{(1)}, \mathbf{n}^{(2)}) &\mapsto (\mathbf{n}^{(1)} - \mathbf{e}_i, \mathbf{n}^{(2)} + \mathbf{e}_i) \text{ with prob. } \frac{cn_i^{(1)}p_2(\mathbf{e}_i|\mathbf{n}^{(1)} - \mathbf{e}_i, \mathbf{n}^{(2)})}{p_1(\mathbf{e}_i|\mathbf{n}^{(1)} - \mathbf{e}_i, \mathbf{n}^{(2)})D(n^{(1)}, n^{(2)})}, \\
(\mathbf{n}^{(1)}, \mathbf{n}^{(2)}) &\mapsto (\mathbf{n}^{(1)} + \mathbf{e}_i, \mathbf{n}^{(2)} - \mathbf{e}_i) \text{ with prob. } \frac{Kcn_i^{(2)}p_1(\mathbf{e}_i|\mathbf{n}^{(1)}, \mathbf{n}^{(2)} - \mathbf{e}_i)}{p_2(\mathbf{e}_i|\mathbf{n}^{(1)}, \mathbf{n}^{(2)} - \mathbf{e}_i)D(n^{(1)}, n^{(2)})},
\end{aligned}$$

for  $i, j \in \{1, 2\}$ .

It remains to specify an approximation for the conditional sampling distribution  $\pi(\cdot|\cdot)$ . This was done for K and W in [SD00], and for TI in [DG04]. A natural approach would be to modify the generator-based method of [DG04] for S as well, but this runs into a problem: because mergers are disallowed in the seed bank, the resulting conditional sampling distribution vanishes for types which are present in the seed bank, but not in the active population. The trunk ancestry method of [PS10] fails for the same reason.

Instead, for the IAM and ISM, we suggest the following modification for sampling the next event given that the current state is  $(\mathbf{n}^{(1)}, \mathbf{n}^{(2)})$ :

- (i) Sample the active or dormant subpopulation with probabilities proportional to

$$\left( n^{(1)} \left( \frac{n^{(1)} - 1}{2} + c + u \right), n^{(2)}(Kc + u') \right).$$

Denote the chosen subpopulation by  $j$ .

- (ii) Sample a lineage uniformly at random from subpopulation  $j$ . Denote its type by  $i$ .

- (iii) With probabilities proportional to

$$\left( \frac{(n_i^{(j)} - 1)^+}{2} \mathbf{1}\{j = 1\}, u\mathbf{1}\{j = 1\} + u'\mathbf{1}\{j = 2\}, c\mathbf{1}\{j = 1\} + Kc\mathbf{1}\{j = 2\} \right),$$

merge the lineage with another one of type  $i$  on island  $j$ , remove from type  $i$  a randomly chosen mutation that does not appear on any other lineage, or migrate the lineage to the other subpopulation. The mutation probability is taken to be 0 if there are no eligible mutations on the lineage, or if the frequency of the allele is greater than one in the case of the IAM.

For the FAM, we suggest pooling the two populations and averaging the rates of mergers and mutations. More precisely, let  $\hat{p}_{SD}(\mathbf{e}_i|\mathbf{n}; u)$  be the approximate conditional sampling distribution of [SD00] for scenario K with mutation rate  $u$ , and define

$$\hat{p}(\mathbf{e}_i|\mathbf{n}^{(1)}, \mathbf{n}^{(2)}) := \hat{p}_{SD}(\mathbf{e}_i|\mathbf{n}^{(1)} + \mathbf{n}^{(2)}; u + u'/K),$$

where the mutation rate has been obtained as the ratio of the average mutation rate,  $uK/(K + 1) + u'/(K + 1)$  and the average merger rate  $K/(K + 1)$ .

## 4 Inference and model selection

In this section we provide an example of the impact of the presence or absence of a seed bank on estimating coalescent parameters from genetic data. We will focus on the population-rescaled mutation rates  $u$  and  $u'$ , but other parameters of interest could be handled similarly. We will also demonstrate that model selection based on full likelihoods is feasible using computationally intensive Monte Carlo techniques.

### 4.1 Estimating the coalescent mutation rate from infinite sites data

The choice of the underlying coalescent model has a large impact on classical estimates of the coalescent mutation rates  $u$  and  $u'$ . The Watterson estimator based on  $S$  observed segregating sites in a sample of size  $n$  is defined as

$$\hat{u}^{\text{K}} := \frac{S}{\mathbb{E}^{\text{K}}[B_n]} \quad \text{resp.} \quad \hat{u}^{\text{W}} := \frac{S}{\mathbb{E}^{\text{W}}[B_n]},$$

for the models  $\{\text{K}, \text{W}\}$ , and where  $B_n$  is the (random) total tree length under each scenario. Since the coalescent under  $\text{W}$  is just a Kingman coalescent in which merger rates are reduced by a factor  $\beta^2$ , we have

$$\mathbb{E}^{\text{W}}[B_n] = \frac{1}{\beta^2} \mathbb{E}^{\text{K}}[B_n],$$

so that given a number of observed segregating sites  $S$ , we expect a lower population-rescaled mutation rate under  $\text{W}$  than under  $\text{K}$ .

For the strong seed bank case  $\text{S}$ , recall from [BGE<sup>+</sup>15, Equation (18)] the relationship

$$\mathbb{E}^{\text{S}}[S] = u\mathbb{E}^{\text{S}}[B_{n_1, n_2}^a] + u'\mathbb{E}^{\text{S}}[B_{n_1, n_2}^d] \quad (6)$$

where  $n := (n_1, n_2)$  is the sample size in the active and dormant populations, respectively, and  $B_{n_1, n_2}^a$  and  $B_{n_1, n_2}^d$  are the (random) total lengths of the active and dormant lines, given the sample size  $n$ .

It is not possible to estimate both mutation rates from the number of segregating sites simultaneously. However, if we assume  $u' = \lambda u$  for some known  $\lambda \geq 0$ , then the following “seed bank Watterson estimator” follows naturally from (6):

$$\hat{u}^{\text{S}} := \frac{S}{\mathbb{E}^{\text{S}}[B_{n_1, n_2}^a] + \lambda \mathbb{E}^{\text{S}}[B_{n_1, n_2}^d]}.$$

A similar estimator can also be defined for the two island model.

The expected branch lengths under all four scenarios are readily available, in closed form under  $\text{K}$  and  $\text{W}$ , and via numerically tractable recursions under  $\text{S}$  and  $\text{TI}$ . Thus, the generalized Watterson estimators above can also be computed. Figure 5 demonstrates the expected branch length profiles under particular choices of parameters. Scenarios  $\text{K}$  and  $\text{W}$  as well as  $\text{S}$  and  $\text{TI}$  resemble one another, as is expected, but it is also clear that an incorrect model choice will result in substantially biased estimates of mutation rates. Different choices of parameters would also lead to different results:

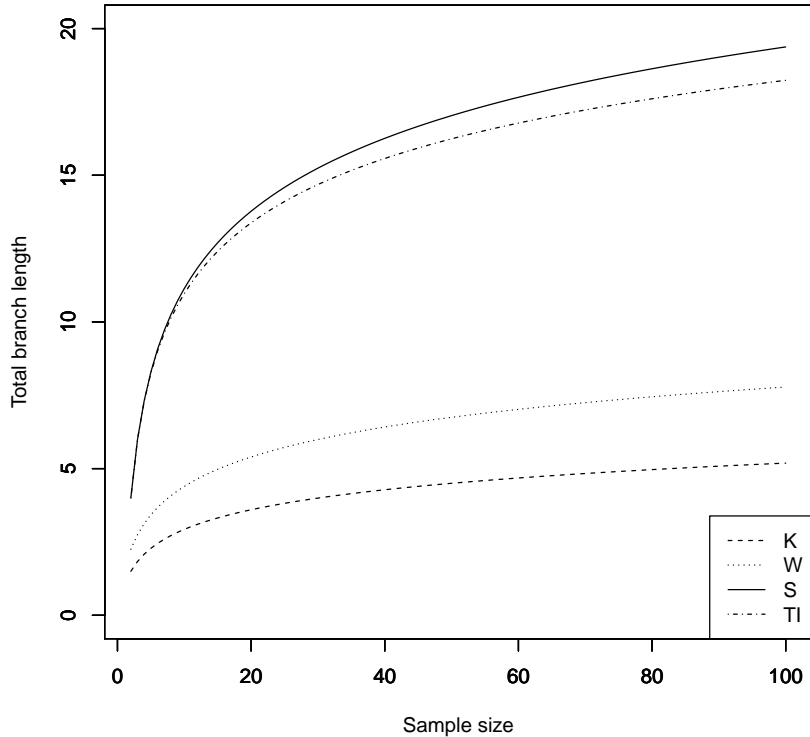


Figure 5: Expected branch lengths as a function of the sample size with  $c = K = 1$  and  $\beta^2 = 1/1.5$ .

for example, taking  $\beta^2 = 1/3.7$  results in a W-curve which lies between the TI and S-curves in Figure 5.

Knowledge of the real substitution rate  $\hat{\mu}$  per year at the (active) locus under consideration allows a real-time embedding of the coalescent history via the relation

$$\text{coalescent time unit} \times \hat{u}^I \approx \text{year} \times \hat{\mu},$$

for  $I \in \{K, W, S, TI\}$ , cf. [EBBF15, Equation (4)] or [SBB13, Section 4.2]. This allows the estimation of quantities such as the time to the most recent common ancestor of a sample in real time, not only in units of coalescent time. In typical cases, one coalescent time unit corresponds to  $O(N)$  generations under all four models considered in this paper.

## 4.2 Model selection based on sampling formulas

We used a pseudo-marginal Metropolis-Hastings algorithm [AR09] to perform full-likelihood model selection and parameter inference simultaneously for models K, S, and TI. Model W was not included as it is not identifiable from K. We focus on the

IMS model in order to balance biological relevance and computational cost. A data set of 100 observed sequences was simulated under each model to act as the observed data. In each case the mutation rate was  $u = 10$ , and for models **S** and **TI** we had  $u' = 0$ ,  $c = K = 1$ , and all 100 sequences were sampled from island 1 to model the impact of an unknown seed bank or population subdivision.

The state space of our pseudo-marginal Markov chain consists of the model indicator  $I \in \{\mathbf{K}, \mathbf{S}, \mathbf{TI}\}$ , as well as the seven non-negative variables

$$\Theta := (u_{\mathbf{K}}, u_{\mathbf{S}}, u_{\mathbf{TI}}, c_{\mathbf{S}}, c_{\mathbf{TI}}, K_{\mathbf{S}}, K_{\mathbf{TI}}).$$

In particular, the fact that  $u' = 0$  under **S** and **TI** was assumed to be known. Given an observed data set  $(\mathbf{t}, \mathbf{n})$ , the target distribution is the posterior

$$q(I, \Theta | \mathbf{t}, \mathbf{n}) \propto p(\mathbf{t}, \mathbf{n} | I, \Theta) q_I(I) q_{u_{\mathbf{K}}}(u_{\mathbf{K}}) \prod_{J \in \{\mathbf{S}, \mathbf{TI}\}} q_{u_J}(u_J) q_{c_J}(c_J) q_{K_J}(K_J),$$

where  $\mathbf{n} = (\mathbf{n}^{(1)}, \mathbf{n}^{(2)})$  in the case of scenarios **S** and **TI**. Here, the likelihood  $p(\mathbf{t}, \mathbf{n} | I, \Theta)$  only charges those coordinates of  $\Theta$  that play a role for model  $I$ , and is flat in all other directions. The prior distributions are  $q_I = (1/3, 1/3, 1/3)$ , and Gamma-distributions with shape parameter 4 for all other variables. Scale parameters are fixed at 1/4 for the  $c$  and  $K$ -variables, and by requiring the prior mean to equal the corresponding Watterson estimator for the  $u$ -variables. This updating of locally redundant variables increases the dimensionality of the model, but also results in faster mixing across the three different models since all parameters are updated simultaneously (see the ‘‘saturated space approach’’ of [BGR09]).

The model index was resampled uniformly at random at each time step, including the possibility of remaining in place. All other parameters were updated using independent Gaussian increments with mean 0 and variance  $\approx 1/14$ , with all parameters being reflected at zero. The importance sampling scheme introduced in Section 3.4 was used to obtain unbiased estimates of likelihoods, with numbers of samples set to 400 for scenario **K**, and 20 000 for scenarios **S** and **TI**. Variances of estimators were further reduced by employing stopping time resampling [Jen12]. These parameters were calibrated so that the log-likelihood estimator variances were close to 3, and acceptance probabilities close to 7%, as shown to be optimal in [STRR15]. C++ code for both simulating observed data sets, and conducting the inference described in this section, is available at GitHub: <https://github.com/JereKoskela/seedbank-infer>.

Three realizations of this Markov chain, one for each simulated data set, were run for 100 000 steps each, initialized from a uniformly chosen model, and the continuous parameters initialized from their respective prior means. The most immediate question is whether each data-generating model can be correctly recovered from its corresponding, observed data set. To that end, posterior probabilities of models are provided in Table 1. It is evident that the true model can be recovered from a moderate amount of data with high confidence, particularly in the case of **K** and **S**.

Also of interest are the posterior distributions of the parameters, given a model class. These are summarized in Figures 6 – 8. None of the parameters are strongly identified, but the posteriors concentrate within a factor of two of the data-generating

True model	$q_I(K \mathbf{t}, \mathbf{n})$	$q_I(S \mathbf{t}, \mathbf{n})$	$q_I(TI \mathbf{t}, \mathbf{n})$
K	0.950	0.042	0.008
S	0.000	1.000	0.000
TI	0.132	0.027	0.841

Table 1: Marginal posterior probabilities of each model class.

parameters, and posterior modes also fall close to these values. Two-dimensional projections of joint posteriors are similarly diffuse, but again center on plausible regions of space (results not shown). The mutation rate is the slowest parameter to mix in all cases, with some residual noise present in the corresponding histograms, while the plots for  $K$  and  $c$  have more clearly converged.

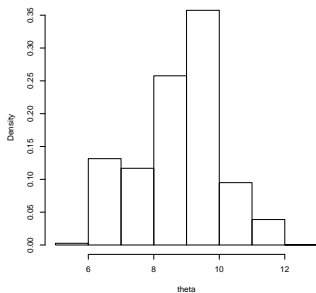


Figure 6: Marginal posterior of  $u_K|I = K$ . Data generated under  $u_K = 10$ .

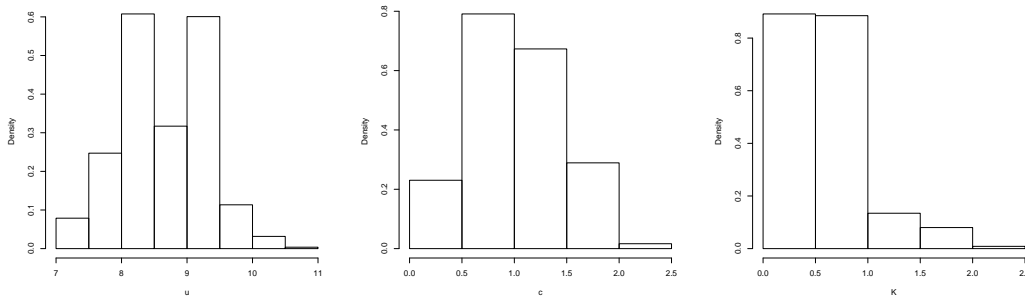


Figure 7: Marginal posteriors of  $(u_S, c_S, K_S)|I = S$ . Data generated under  $(u_S, c_S, K_S) = (10, 1, 1)$ .

While the method presented in this section is computationally intensive and cannot be expected to scale to large data sets, it does set a benchmark for what we may expect of the performance of more scalable methods. In particular, the three model classes ought to be distinguishable with high confidence (or moderate confidence in the case of TI), but precise values of parameters within model classes are challenging to pinpoint without strong prior information, or data from multiple unlinked loci.

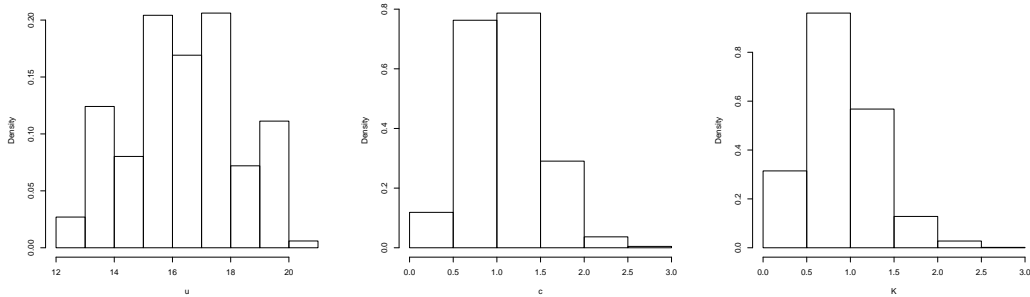


Figure 8: Marginal posteriors of  $(u_{\text{TI}}, c_{\text{TI}}, K_{\text{TI}}) | I = \text{TI}$ . Data generated under  $(u_{\text{TI}}, c_{\text{TI}}, K_{\text{TI}}) = (10, 1, 1)$ .

### 4.3 Detecting mutation in the seed bank

In this section we focus on a different model selection problem: whether mutation is taking place in a strong seed bank that is known to be present. Data sets were simulated under two scenarios:

S1. Model **S** with  $u = 10, u' = 0$ .

S2. Model **S** with  $u = u' = 5$ .

All other parameters and simulation details are as in Section 4.2. A pseudo-marginal Metropolis-Hastings chain was run targeting these two hypotheses, with the same priors as in Section 4.2. In scenario S1 we assumed that  $u' = 0$  was known, while in scenario S2 we assumed that  $u = u'$  was known, but that the common value itself was not. The posterior probabilities of each scenario are given in Table 2.

True scenario	$q_I(S1   \mathbf{t}, \mathbf{n})$	$q_I(S2   \mathbf{t}, \mathbf{n})$
<b>S1</b>	1.000	0.000
<b>S2</b>	0.098	0.902

Table 2: Marginal posterior probabilities of each scenario.

It is evident that the presence or absence of mutation in a seed bank can be detected with high confidence from a modest amount of data. Figures 9 and 10 below show that parameters remain relatively weakly identified, particularly in the case of mutation rates, which were also the slowest parameters to mix.

## 5 Discussion

We have reviewed several population genetic models related to seed banks, in combination with several classical mutation models. We derived expressions for classical

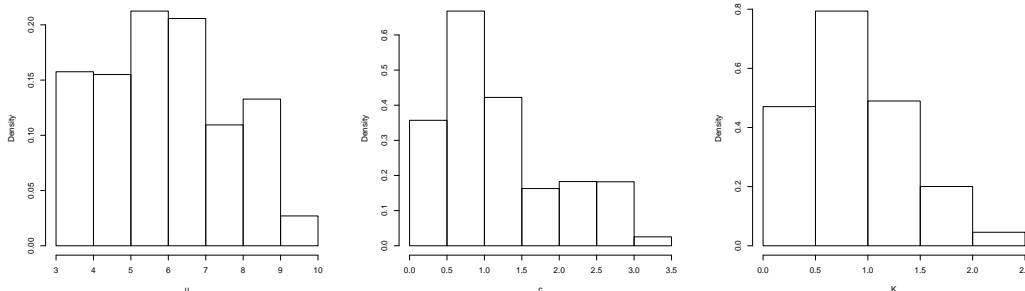


Figure 9: Marginal posteriors of  $(u, c, K)|I = \text{S1}$ . Data generated under  $(u, u', c, K) = (10, 0, 1, 1)$ .

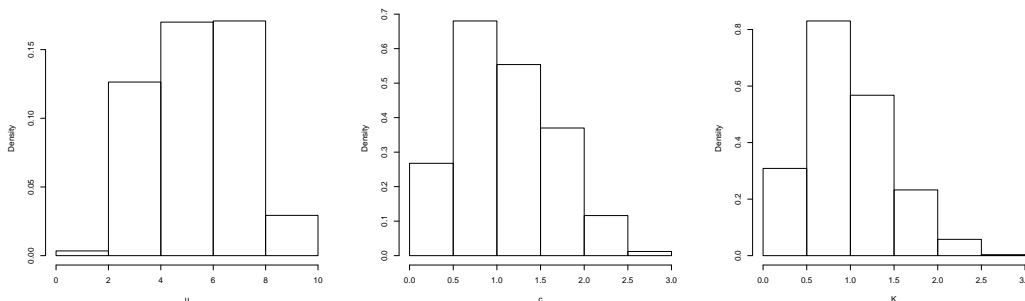


Figure 10: Marginal posteriors of  $(u, c, K)|I = \text{S2}$ . Data generated under  $(u, u', c, K) = (5, 5, 1, 1)$ .

population genetic summary statistics such as the  $F_{ST}$  and the SFS for various suitable combinations of coalescent and mutation models. We then studied and summarized the identifiability of various scenarios and parameters based on either tractable summary statistics, or computationally intensive full likelihood methods.

While weak seed banks cannot be detected via the  $F_{ST}$  in the two alleles case, the strong seed bank scenario produces elevated levels of  $F_{ST}$ , which are also smaller than those of the two-island model with otherwise identical parameters. The signal is slightly stronger in the case without mutation in the seed bank compared to the case with mutation, but generally appears to be too weak to allow for confident detection of a strong seed bank. Explicit (yet much more involved) expressions for the  $F_{ST}$  results can also be obtained in the infinite alleles and infinite sites models, using phase-type distribution arguments as in [HSJB18] and yield a similar picture.

Considering the normalized SFS instead of  $F_{ST}$  results in improved statistical power. The Kingman and the weak seed bank scenarios can only be distinguished with prior knowledge of the population-rescaled mutation rate(s), whereupon the number of expected segregating sites suffices as a statistic. The strong seed bank and two island models result in an excess of singletons and a lighter tail in the nSFS when compared to the classical Kingman case, for sample sizes as low as  $n = 8$ . Thus, these two scenarios can be distinguished from K and W, but not from each other.

To study the scope of possible inference, we used a Monte Carlo scheme to approximate full sampling likelihoods under various scenarios. Model selection from simulated data gives good results for samples of size  $n = 100$ , even in the presence of parameter uncertainty. Accounting for parameter uncertainty in the simulation pipeline is particularly important, because standard estimators such as the Watterson estimator assume a fixed coalescent model, and thus using the wrong estimator can strongly bias further inferences, as well as the corresponding real-time embedding of the results. We also demonstrated that our method is able to detect whether mutation is taking place in the seed bank, again in the presence of parameter uncertainty. Thus, it provides a promising first step towards answering such questions in general [LJ11].

Our paper is a starting point for the statistical methodology for seed bank detection. We have shown that model selection and inference are possible from moderate data sets in principle, but several important points remain to be addressed.

First, the adequacy and universality of the models needs to be established. They all describe idealized scenarios in population genetics, with constant population sizes, and in the absence of further evolutionary forces such as selection. The effect of such forces in the presence of seed banks remains unknown, and may confound some or all of the results we have presented.

Second, the type of seed bank formation mechanism itself needs to be discussed. The strong seed bank model of [BGKW16] follows the modeling idea of [LJ11], where switching happens on an individuals basis. This model corresponds to “spontaneous switching” of bacteria and might be appropriate for populations in “stable” environments [LJ11]. However, in real populations initiation of or resuscitation from dormancy can be triggered by environmental cues, and in such situations it is plausible that many individuals switch their state simultaneously. This leads to a scaling regime that is different from the migration-type behavior of the strong seed bank model (and of course also differs from the weak seed bank model of [KKL01]). Here, one expects to obtain coalescent models with simultaneous activation and deactivation of lineages (so-called “on/off-coalescents”), and the derivation of suitable models and scaling limits is currently under active mathematical research [BGKW19].

**Acknowledgement.** JB and MWB supported (in part) by DFG Priority Programme 1590 “Probabilistic Structures in Evolution”, project 1105/5-1, EB supported by DFG RTG 1845 and BMS Berlin Mathematical School, JK supported in part by EPSRC grant EP/R044732/1.

## References

- [AR09] C. Andrieu and G. O. Roberts. The pseudo-marginal approach for efficient Monte Carlo computations. *Ann Stat*, 37:697–725, 2009.
- [ASS07] U. Arunyawat, W. Stephan, and T. Städler. Using multilocus sequence data to assess population structure, natural selection, and linkage disequilibrium in wild tomatoes. *Mol. Biol. and Evol.*, 24(10):2310–2322, 2007.

- [BB08] M. Birkner and J. Blath. Computing likelihoods for coalescents with multiple collisions in the infinitely many sites model. *J. Math. Biol.*, 57(3):435–465, 2008.
- [BBGW19] J. Blath, E. Buzzoni, A. González Casanova, and M. Wilke-Berenguer. Structural properties of the seed bank and the two island diffusion. *J. Math. Biol.*, 79(1):369–392, 2019.
- [BGE<sup>+</sup>15] J. Blath, A. González Casanova, B. Eldon, N. Kurt, and M. Wilke-Berenguer. Genetic variability under the seedbank coalescent. *Genetics*, 200(3):921–934, 2015.
- [BGKS13] J. Blath, A. González Casanova, N. Kurt, and D. Spanò. The ancestral process of long-range seed bank models. *J. Appl. Probab.*, 50(3):741–759, 2013.
- [BGKW16] J. Blath, A. González Casanova, N. Kurt, and M. Wilke-Berenguer. A new coalescent for seed-bank models. *Ann. Appl. Probab.*, 26(2):857–891, 2016.
- [BGKW19] J. Blath, A. González Casanova, N. Kurt, and M. Wilke-Berenguer. The seed bank coalescent with simultaneous switching. *arXiv:1812.03783*, 2019.
- [BGR09] S. P. Brooks, P. Giudici, and G. O. Roberts. Efficient construction of reversible jump Markov chain Monte Carlo proposal distributions. *J R Stat Soc B*, 65:3–55, 2009.
- [DG04] M. De Iorio and R. C. Griffiths. Importance sampling on coalescent histories II: Subdivided population models. *Adv. in Appl. Probab.*, 36(2):434–454, 2004.
- [dHP17] F. den Hollander and G. Pederzani. Multi-colony Wright-Fisher with seed-bank. *Indag. Math. (N.S.)*, 28(3):637–669, 2017.
- [EBBF15] B. Eldon, M. Birkner, J. Blath, and F. Freund. Can the site-frequency spectrum distinguish exponential population growth from multiple-merger coalescents? *Genetics*, 199(3), 2015.
- [EK86] S. N. Ethier and T. G. Kurtz. *Markov processes*. Wiley Series in Probability and Mathematical Statistics: Probability and Mathematical Statistics. John Wiley & Sons, Inc., New York, 1986. Characterization and convergence.
- [Eth11] A. Etheridge. *Some mathematical models from population genetics*, volume 2012 of *Lecture Notes in Mathematics*. Springer, Heidelberg, 2011. Lectures from the 39th Probability Summer School held in Saint-Flour, 2009, École d’Été de Probabilités de Saint-Flour. [Saint-Flour Probability Summer School].
- [HC97] D. L. Hartl and A. G. Clark. *Principles of population genetics*, volume 116. Sinauer associates Sunderland, MA, 1997.

- [Her94] H. M. Herbots. *Stochastic models in population genetics: genealogical and genetic differentiation in structured populations*. PhD thesis, University of London, 1994.
- [HL66] J. L. Hubby and R. C. Lewontin. A molecular approach to the study of genic heterozygosity in natural populations. I. the number of alleles at different loci in *Drosophila Pseudoobscura*. *Genetics*, 54(2):577–594, 1966.
- [HSJB18] A. Hobolth, A. Siri-Jégousse, and M. Bladt. Phase-type distributions in population genetics. *arXiv preprint arXiv:1806.01416*, 2018.
- [Jen12] P. A. Jenkins. Stopping-time resampling and population genetic inference under the coalescent model. *Stat Appl Genet Mol*, 11:Article 9, 2012.
- [Kin82] J. F. C. Kingman. The coalescent. *Stoch Proc Appl*, 13:235–248, 1982.
- [KKL01] I. Kaj, S. M. Krone, and M. Lascoux. Coalescent theory for seed bank models. *J. Appl. Probab.*, 38:285–300, 2001.
- [LJ11] J. T. Lennon and S. E. Jones. Microbial seed banks: the ecological and evolutionary implications of dormancy. *Nat. Rev. Microbiol.*, 9(2):119–130, 2011.
- [Not90] M. Notohara. The coalescent and the genealogical process in geographically structured population. *Journal of mathematical biology*, 29(1):59–75, 1990.
- [PS10] J. S. Paul and Y. S. Song. A principled approach to deriving approximate conditional sampling distributions in population genetic models with recombination. *Genetics*, 186:321–338, 2010.
- [SBB13] M. Steinruecken, M. Birkner, and J. Blath. Analysis of dna sequence variation within marine species using beta-coalescents. *Theor Pop Biol*, 87:15–24, 2013.
- [SD00] M. Stephens and P. Donnelly. Inference in molecular population genetics. *J. R. Statist. Soc. B*, 62(4):605–655, 2000.
- [SL18] W. R. Shoemaker and J. T. Lennon. Evolution with a seed bank: the population genetic consequences of microbial dormancy. *Evol Appl.*, 11(1):60–75, 2018.
- [STRR15] C. Sherlock, A. Thiery, G. O. Roberts, and J. S. Rosenthal. On the efficiency of pseudo-marginal random walk Metropolis algorithms. *Ann Stat*, 43:238–275, 2015.
- [TLL<sup>+</sup>11] A. Tellier, S. J. Y. Laurent, H. Lainer, P. Pavlidis, and W. Stephan. Inference of seed bank parameters in two wild tomato species using ecological and genetic data. *Proc. Natl. Acad. Sci. U.S.A.*, 108(41):17052–17057, 2011.

- [VRP00] R. H. Vreeland, W. D. Rosenzweig, and D. W. Powers. Isolation of a 250 million-year-old halotolerant bacterium from a primary salt crystal. *Nature*, 407:897–900, 2000.
- [Wak09] J. Wakeley. *Coalescent Theory: An Introduction*. Coalescent theory: an introduction. Roberts & Company Publishers, Greenwood Village, 2009.
- [Wri51] S. Wright. The genetical structure of populations. *Ann. Eugen.*, 15(1):323–354, 1951.
- [ZT12] D. Zivković and A. Tellier. Germ banks affect the inference of past demographic events. *Molecular ecology*, 21(22):5434–5446, 2012.